

Highlights

1. Glacial geomorphology and geochronology of South Georgia described from swath bathymetry
2. Consistent pattern of large scale submarine geomorphological features observed in fjords
3. Last Glacial Maximum restricted to inner fjords
4. Cross shelf troughs, and moraines document more extensive pre-LGM glaciations
5. Glacial history similar to that of central Patagonia

1 **Glacial history of sub-Antarctic South Georgia based on the**
2 **submarine geomorphology of its fjords**

3

4 Dominic A. Hodgson^{1*}, Alastair G.C. Graham^{1,2*}, Huw J. Griffiths¹, Stephen J.
5 Roberts¹, Colm Ó Cofaigh³, Michael J. Bentley³, David J.A. Evans³

6

7 ¹British Antarctic Survey, High Cross, Madingley Road, Cambridge, CB3 0ET, UK

8 ²Now at: School of Geography, College of Life and Environmental Sciences,
9 University of Exeter, Amory Building, Rennes Drive, Exeter, EX4 4RJ, UK

10 ³Department of Geography, Durham University, South Road, Durham, DH1 3LE, UK

11

12 Author for correspondence: daho@bas.ac.uk

13 *These authors contributed equally to this research

14

15 **Abstract**

16 We present multibeam swath bathymetric surveys of the major fjords surrounding the
17 sub-Antarctic island of South Georgia to characterise the glacial geomorphology and
18 to identify the relative timings and extent of past glacial advance and retreat.

19 Bathymetry data revealed a range of glacial features including terminal, retreat and
20 truncated moraines, deep (distal) outer and shallow (proximal) inner basins and cross
21 shelf troughs. These provide evidence of glacial advance and retreat through several
22 glacial cycles. A relatively consistent pattern of large scale submarine
23 geomorphological features was observed in the different fjords suggesting a similar
24 response of margins of the island ice cap to past climate forcing. A relative
25 chronology based on the relationships between the submarine features with their

26 radiocarbon and cosmogenic isotope dated terrestrial counterparts suggests that
27 widely observed inner basin moraines date from the last major glacial advance or Last
28 Glacial Maximum, while deep basin moraines may date from an earlier (pre-LGM)
29 more extensive glaciation, which we speculate corresponds to MIS6. On the sides of
30 the deep basin troughs a series of truncated moraines show ice advance positions from
31 preceding glacial periods. The cross shelf troughs, and mid-trough moraines are
32 interpreted as the product of much more extensive pre-LGM glaciations that predate
33 the fjord geomorphology mapped here, thus possibly older than MIS6. This
34 hypothesis would suggest that South Georgia followed a glacial history similar to that
35 of central Patagonia (46°S) where a series of Pleistocene glaciations (of MIS 20 and
36 younger) extended beyond LGM limits, with the most extensive glacial advance
37 occurring at *c.* 1.1 Ma.

38

39

40

41 **1. Introduction**

42 South Georgia is situated between the Antarctic Peninsula and southernmost South
43 America. Its glacial history has been studied for nearly a century (Gregory, 1915).
44 The main research questions have focused on whether its glaciations are in phase or
45 out of phase with the South American, Antarctic and northern hemisphere glaciations,
46 defining the maximum ice extent during the last glacial cycle, and establishing a
47 chronology for deglaciation and glacier fluctuations during the Holocene. All of these
48 questions have the wider goal of improving our understanding of the mechanisms of
49 climate change, both regionally and with respect to the phasing of climate changes
50 between the hemispheres (Broecker, 1998), as well as improving understanding of the
51 mechanisms of ice sheet decay and its impact on global sea levels (Sugden, 2009).

52

53 To date, glacial geomorphological research on South Georgia has focused on the
54 terrestrial geomorphology which has established that an independent ice cap glaciated
55 the island during the local Last Glacial Maximum (referred to hereafter simply as
56 'LGM') (Clapperton, 1971; Sugden and Clapperton, 1977; Clapperton and Sugden,
57 1988; Clapperton et al., 1989; Bentley et al., 2007). Most of the effort has been
58 focussed on interpreting the glacial features in specific, and logistically more
59 accessible, locations on the basis of comparative geomorphology and
60 geomorphological mapping (Clapperton, 1971; Stone, 1974; Clapperton et al., 1989),
61 radiocarbon-based geochronological models of glacial sediments (Gordon, 1987),
62 combined radiocarbon and cosmogenic isotope dating of moraines (Bentley et al.,
63 2007), the onset of sedimentation in lakes and peat bogs (Clapperton et al., 1989;
64 Wasell, 1993; Rosqvist et al., 1999; Rosqvist and Schuber, 2003; Van der Putten et
65 al., 2004; Van der Putten, 2008), and lichenometric studies (Roberts et al., 2010).

66 More recently the remarkable maximum extent of past glaciations around South
67 Georgia has been revealed by a new compilation of bathymetric soundings from the
68 continental shelf and surrounding waters. This has revealed large cross shelf glacial
69 troughs, moraines and trough mouth fans on the shelf and slope at an unprecedented
70 level of detail (Graham et al., 2008; Fretwell et al., 2009). These suggest that one or
71 more glaciations have extended to the continental shelf break. Collectively, these
72 studies have considerably advanced our understanding of the glacial history, but it is
73 still not known whether at the LGM the ice cap extended to the edge of the
74 continental shelf around South Georgia (Clapperton et al., 1989), or if the LGM was
75 limited to the inner fjords as suggested both by the more recent mapping and dating of
76 the onshore Late Glacial to Holocene moraines (Bentley et al., 2007), and by the
77 deposition of lake sediments indicating ice free conditions from 18,572 cal. yrs BP
78 (Rosqvist et al., 1999). The former theory would suggest that the glacial history of
79 South Georgia is an analogue to the glacial record on the Antarctic Peninsula, where
80 the ice sheet and its discharging glaciers extended to the shelf break at the LGM, and
81 subsequently retreated in a stepwise pattern to the present. The latter theory would
82 require the LGM to follow a glacial history similar to that of central Patagonia (46°S)
83 where a series of Pleistocene glaciations (of MIS 20 and younger) extended beyond
84 LGM limits (Rabassa, 2000), with the most extensive glacial advance occurring *c.* 1.1
85 Ma (Singer et al., 2004).

86 At present the accumulated data on the glacial geomorphology of South Georgia lacks
87 a detailed examination of the submarine geomorphology of the inner fjords and bays
88 which form the gateways to the prominent deep cross-shelf troughs. Such information
89 can often provide exceptionally well-preserved evidence of glacial geomorphology
90 that can be matched to the record on land. Fjords are glacially over-deepened, semi-

91 enclosed marine basins, that often preserve evidence of environmental change in their
92 geomorphology and sediments (Howe et al., 2010). Most fjords have been glaciated a
93 number of times and many of those on South Georgia still possess a resident tidewater
94 glacier (where the terminus is grounded below sea level (Cook et al., 2010)). The
95 submarine geomorphology of many fjords can provide evidence of the advance and
96 retreat of glaciers and in some cases the limits of former glaciations. Fjords can also
97 accumulate sediment archives from which the timing of glaciation timing and post-
98 glacial environmental changes can be deduced (Howe et al., 2010). The aim of this
99 paper was therefore to carry out detailed marine geophysical surveys of the South
100 Georgia fjords, to describe their geomorphology and from this, to interpret their
101 glacial history. This fills an important gap between the recent studies of palaeo-ice
102 sheet drainage on the continental shelf (Graham et al., 2008) and the glacial
103 geomorphology and chronology of ice-cap deglaciation on land from the last glacial
104 cycle (Bentley et al., 2007). From this data set a new chronology of glaciations on
105 South Georgia is proposed together with a rationale for selecting sediment coring sites
106 in the fjords to further test which theory regarding the deglacial chronology of South
107 Georgia since the LGM is correct.

108

109 1.1 Study area

110 South Georgia (Fig. 1) has been described in detail in recent papers (Bentley et al.,
111 2007; Gordon et al., 2008; Graham et al., 2008; Fretwell et al., 2009). The island is
112 part of the North Scotia Ridge and lies ~350 km south of the Antarctic Polar Frontal
113 Zone (54–55°S, 36–38°W) (Fig. 1A). The most prominent relief consists of two
114 mountain ranges that form an elongate NW-SE chain, 175 km-long and 2 to 35 km
115 wide reaching up to 2935 m a.s.l (Fig. 1B). The mountains are heavily glaciated with

116 series of ice fields feeding glaciers that terminate either on land or, more commonly,
117 into the sea via steep sided bays and u-shaped fjords. These bays and fjords dissect the
118 coastline to the north and south of the island and then extend into major glacial cross-
119 shelf troughs which radiate 40-102 km out towards the edge of the continental shelf
120 (Graham et al., 2008). The climate is maritime. Mean annual temperature at
121 Grytviken, on the more sheltered north coast is c. 1.7 °C, with an annual precipitation
122 at sea level of c.1395 mm, but is highly variable on account of the island's position
123 near the Antarctic sea ice limit, the behaviour of the Antarctic Circumpolar Current
124 and related deep water tongues, which influence the island to its east and north, and
125 frequent depressions driven by the southern hemisphere westerly winds. These
126 physiographic conditions result in a highly sensitive glaciological regime that has
127 been shown to respond rapidly to changes in temperature and precipitation (Gordon et
128 al., 2008; Cook et al., 2010). The most deglaciated areas are the peninsulas on the
129 north coast. These are where most terrestrial studies have been carried out to-date.

130

131

132 **2. Methods**

133

134 Multibeam swath bathymetric surveys of selected fjords were carried out in 2005 and
135 2006 using a high-resolution shallow-water Kongsberg EM710S multibeam echo
136 sounder on HMS *Endurance*. We combined these new data sets with existing data
137 collected using a deep-water Kongsberg EM120 multibeam echo sounder on various
138 cruises of the RRS *James Clark Ross* to the South Georgia region. Both echo
139 sounders are 1 x 1° resolution systems; the EM710S acquires 400 soundings per
140 swath at 70-100 kHz, while the EM120 acquires data across a fan of 191 beams at

141 11.25–12.75 kHz. Practical port- and starboard-side angles of up to ~68° provided a
142 sea-floor coverage of c. 4-5 times water depth. Data from the former are archived at
143 the UK Hydrographic Office, and for the latter in the NERC Polar Data Centre. All
144 multibeam data were ping-edited and gridded together using tools in the UNIX-based
145 MB-System (Caress & Chayes 2006, [http://www.ldeo.columbia.edu/res/pi/MB-](http://www.ldeo.columbia.edu/res/pi/MB-System)
146 [System](http://www.ldeo.columbia.edu/res/pi/MB-System)). Navigational data were recorded using differential GPS receivers. Sub-
147 bottom topographic parametric sonar (TOPAS) data were acquired in Cumberland
148 Bay, on the north coast of South Georgia (Fig. 1A), during cruise JR224 of the RRS
149 *James Clark Ross*, using a Kongsberg Simrad TOPAS PS018 sub-bottom profiler
150 operated in ‘chirp’ mode. Because such data have not been collected routinely in
151 previous cruises to the South Georgia shelf, sub-bottom data were limited to only a
152 small number of transects in this single fjord.

153

154 Cleaned data sets were gridded at high resolution to enhance the imaging of subtle
155 submarine features. For most of the study area, we produced gridded datasets with
156 cell sizes ranging from 4-10 m, suitable for the range of water depths encountered in
157 the fjord regions (50-300 metres). Two of the bathymetric grids (Drygalski Fjord and
158 King Haakon Fjord) were derived from existing gridded single-beam surveys, using
159 legacy data provided by UK Hydrographic Office. Consequently, bathymetric
160 resolution is lower in these areas compared to the fjords to the north of the island
161 (>12-15 m). Nevertheless, glacial geomorphic features are still distinguishable on
162 these datasets.

163

164 Vertical accuracy of both the multibeam and singlebeam systems are dependent on
165 acquisition factors, but in shallow depths uncertainty normally equates to better than 1

166 metre (0.2% of the water depth across the entire swath). Bathymetric data are
167 presented as plan and oblique shaded-relief images to differentiate the major sea-floor
168 landforms.

169

170 Cross sections were taken through key features such as moraines, fjord basins, and
171 debris cones. The offshore data were combined with near-shore satellite images of
172 South Georgia (a compilation of SIO, NOAA, U.S. Navy, NGA and GEBCO sources)
173 and with previously published onshore geomorphological maps (Bentley et al., 2007)
174 (see figures in Appendix A) to highlight the relationships between the submarine
175 fjord, and known terrestrial geomorphology.

176

177

178 **3. Results**

179

180 Surveys of the fjords that dominate the South Georgia coastline were carried out on
181 the major inlets along the northern coast of the islands, together with accessible fjords
182 on the south west and east coasts. The survey regions are shown as numbered boxes
183 on a regional bathymetric map of the South Georgia continental shelf (Fig. 1, Fretwell
184 et al., 2009). This shows the relationship of the surveyed fjords to the trough systems
185 on the continental shelf. The submarine surveys revealed a range of glacial land forms
186 from which the interrelationships between different features in each fjord could be
187 examined. The results of the individual fjord surveys are described below.

188

189 **3.1 Royal Bay**

190 Royal Bay (Fig. 2) is a 241 m deep fjord, occupied until recently by the combined
191 Ross/Hindle Glaciers, which have now divided and discharge separately into the bay
192 from the south and the west (Fig. 2A). The bay is also fringed by a minor tidewater
193 glacier, the Weddell Glacier that discharges into it from the south (located south of
194 the red star in Fig. 2A). The Weddell Glacier terminates in a small embayment
195 partially enclosed by a terminal moraine or shingle spit formed by reworking of
196 glacial deposits. The fjord is approximately 12 km long and broadens in width
197 seaward from 4 to 7.5 km before it extends beyond the headlands of Harcourt Island
198 to the north and Cape Charlotte to the south (Fig. 2). The fjord consists of a relatively
199 shallow inner basin whose modern-day topography is likely the result of a high
200 sediment flux at the glacier terminus. The inner basin extends eastwards to a
201 prominent c. 10-25 m-high transverse moraine ridge which has been partially
202 breached on its northern side and towards the centre of the fjord (Fig. 2F). The top of
203 the ridge, and the breaches, are interpreted to have been shaped by past interactions
204 with icebergs shed from the nearby tidewater glacier fronts, likely when the glaciers
205 were grounded in greater water depths, in a more advanced position. The unusual
206 surface morphology on the steep distal flank of the moraine is also reminiscent of
207 features composed of stacked thrust blocks, and suggests that the moraine may have
208 formed by the thrusting and deformation of fjord sediments as the glacier advanced to
209 this moraine limit. Beyond the inner basin moraine, the fjord extends into a deep
210 smooth-bottomed, probably sediment-filled deep basin. On the north side of this deep
211 outer basin are four clear promontories, which are interpreted as truncated moraines.
212 It is possible that they are matched by the similar but less distinct features on the
213 southern flank of the trough (Fig. 2C, D). Hummocky lobes at the foot of some of
214 these truncated features are considered the result of rock fall which could have occurred

215 after the last glacier terminus in the deep trough retreated landward of these moraines.
216 Other notable features in the fjord are a relict meltwater channel that probably issued
217 from a subglacial conduit at the northern part of the Ross Glacier front in the recent
218 past, forming a chute with levees, carved into the seaward flank of the fjord floor
219 where it shallows towards the coast (perhaps representing another moraine ridge near
220 the terminus of the glacier, or the fjord bedrock) (Fig. 2E, 3). Seaward of the chute are
221 a series of small, slightly sinuous ridges and intervening channels, oriented broadly
222 parallel to the modern glacial front. There are several possible interpretations for these
223 features: they may be a series of abandoned channels which together have discharged
224 sediment gravity flows into the inner basin, their morphology reflecting sediment
225 creep and deflection to the south by the Coriolis Effect (Fig. 3). Alternatively, the
226 ridges can be interpreted as a series of small recessional moraines, stacked behind a
227 curvi-linear ridge that is a larger end moraine. In either case, there appears to be
228 evidence in Royal Bay for active or recently-active subglacial fluvial transport,
229 including a possible esker ridge system that lies immediately south of the small ridge
230 set (Fig. 3). Rapid sedimentation from the jet and plume as a subglacial meltwater
231 channel issues from the grounding line is a common process in temperate and sub-
232 polar, glacier-influenced fjords (Pfirman and Solheim, 1989; Powell and Alley, 1997;
233 Ó Cofaigh and J.A., 2001) and is the most likely source of the sediments that fill both
234 the inner and outer fjord basins.

235

236 3.2 Cumberland Bay East

237 The Cumberland Bay complex is the largest fjord system on South Georgia and is the
238 outlet for the major glaciers of the Allardyce Range and the Kohl Plateau Ice Field.
239 Cumberland Bay East (Fig. 4) is approximately 15 km long, 3-5 km wide and up to

240 270 m deep, extending from the terminus of the Nordenskjöld Glacier to Sappho Point
241 where it merges with Cumberland Bay West and connects to the head of a prominent
242 cross shelf trough (Fig. 1, 4A). It consists of one principal fjord with two tributary
243 fjords: Moraine Fjord and King Edward Cove (KEC on Fig. 4A). Moraine Fjord is a 6
244 km long re-entrant and the outlet for two tidewater glaciers, the Hamberg Glacier and
245 Harker Glacier whilst King Edward Cove is not currently glacierised. The mouth of
246 Moraine Fjord is enclosed by an arcuate submarine terminal moraine, most likely an
247 extension of a laterofrontal moraine complex described by Bentley et al. (2007)
248 whose large boulders and kelp beds are exposed at low tide, whilst King Edward
249 Cove is partially enclosed by a shingle spit: King Edward Point. Like Royal Bay,
250 Cumberland Bay East consists of a relatively shallow inner basin terminating in a
251 prominent inner basin moraine which is well-preserved on the north side but has
252 multiple breaches in the centre of the fjord (Fig. 4B). Because of their highly random
253 orientations these breaches are likely to have been caused by iceberg ploughing.
254 Ploughing of the sediment by icebergs is evident in circular grounding pits and
255 chaotic scours that are present in water shallower than ~220 m depth, near the
256 terminus of the Nordenskjöld Glacier. Because the sea-floor deepens slightly away
257 from the coast here, the scours can only feasibly have formed during episodes of
258 terminus retreat from a more extensive position. As is the case with Royal Bay, the
259 fjord deepens seaward to an outer basin 270 m deep, immediately seaward of the
260 inner basin moraine. Again, there are a series of potential truncated moraines or
261 submarine bedrock promontories, one of which lies approximately 1 km northeast of
262 King Edward Cove (Fig. 4A), and is likely a relict moraine formed by an extended
263 Hamberg/Harker Glacier occupying Moraine Fjord. At the mouth of the fjord there is
264 a second moraine marking the outer limit of the deep basin. This appears partly

265 eroded and breached near the centre of the fjord, although well preserved otherwise
266 (Fig. 4C). There is a series of topographic highs between this moraine and Barff Point
267 (Right Whale Rocks) which may be truncated moraines, and an unusual,
268 discontinuous sea-bed high landward of the moraine, which is possibly a remnant
269 moraine owing to the fact that it shares a cross-profile similar to that of the outer-
270 basin moraine (Fig. 4D, 4E). Other notable features on land are the outwash from the
271 fjord valley system of the Hamberg ‘valley’ and Moraine Fjord, separated by a
272 moraine complex, Zenker Ridge, which formed along the northwest margin of the
273 expanded Harker Glacier and extended offshore from the mouth of Moraine Fjord.
274 The adjacent Hamberg Valley (HV on Fig 4A) has most likely been formed by a fjord
275 becoming infilled with glaciofluvial sediment to above sea level, assisted by post
276 glacial isostatic rebound and relative sea level fall. The floor of this paraglacial
277 coastal valley, Hesterletten (HS on Fig 4 A), comprises reworked glacial sediment
278 with a prograding fjord head delta and braided river system with a trunk stream that
279 has discharged sediments into Cumberland Bay East via turbidity currents and
280 sediment plumes. These sediments extend up to 3 km into the bay. Multiple slope
281 failures can be seen in this reworked glacial sediment immediately seaward of the
282 Hamberg Valley. Small slope failures are also present at various locations along the
283 margins of Cumberland Bay East where a deep sedimentary infill is evident on
284 TOPAS sub-bottom profiler data (e.g. Fig. 4E).

285

286 3.3 Cumberland Bay West

287 Cumberland Bay West (Fig. 5) is the outlet for the Neumayer and Geikie glaciers and
288 the heavily debris covered Lyell Glacier. All three are tidewater glaciers with the
289 Neumayer Glacier discharging directly into Cumberland Bay West and the Lyell and

290 Geikie Glaciers discharging into tributary fjords, Harpon Bay and Mercer Bay, which
291 are both partially enclosed by moraines exposed as kelp beds at low tide. Cumberland
292 Bay West is approximately 18 km long and 2.5-5 km wide and up to 265 m deep,
293 extending to Mai Point beyond which it merges with Cumberland Bay East (Fig 4A).
294 Mapping of the fjord did not extend to the glacier fronts so we did not identify a
295 shallow inner basin moraine, although from Admiralty Chart 3597 (South Georgia)
296 and the compilation data in Fig 1a., it is possible that it may occur just south of Carlita
297 Bay where Bentley et al. (2007) document a series of moraines associated with an
298 earlier advance of the Neumayer Glacier (Appendix Fig. A2). From the survey limits,
299 the fjord deepens seaward past a series of up to four submerged promontories,
300 possibly truncated moraines, to a heavily eroded outer moraine which shares a similar
301 profile to the outer basin moraine in Cumberland Bay East (Fig. 5C), and is eroded
302 away on the central and southern parts of the fjord (Fig. 5B). Other notable features
303 are debris cones or moulin kames, interpreted to have formed where sediment-laden
304 water and/or supraglacial debris has drained through or melted out of sink holes in the
305 floating glacier when it occupied a more advanced position in the fjord. There is also
306 a possible medial moraine extending seaward from Middle Head (Fig. 5A).

307

308 3.4 Stromness Bay and Husvik Bay

309 Stromness Bay and Husvik Bay (Fig. 6) are two shallow fjords 6-8 km long
310 (measured to the deep basin moraine, Fig. 6B), up to 2.5 km wide and approximately
311 50-160 m deep, separated by Tonsberg Point (Fig. 6A). Tidewater glaciers are absent
312 from these fjords, which are currently amongst the most deglaciated parts of the
313 island. As with the other fjords the general pattern of a shallow inner basin
314 terminating in a shallow, flat-topped moraine is repeated. In this case the inner basin

315 consists of a complex of basins that have originated from earlier glaciers occupying
316 the three major glacial valleys feeding into Leith, Stromness and Husvik Bays. The
317 inner basin moraine is located just beyond Tonsberg Point in Husvik Bay and
318 immediately south of Black Rocks in Stromness Bay (Fig. 6C). This observation
319 suggests formation by two independent glaciers, because the inner basin moraines do
320 not form one continuous ice-marginal limit. The moraine in Stromness Bay has a deep
321 breach in the centre of the fjord. Three lateral or frontal moraines derived from valley
322 glaciers in Leith and Husvik harbours are present between Berntson Ridge and Grass
323 Island and similar features are present in Husvik Bay. Elsewhere it is difficult to
324 separate moraines from bedrock features. From terrestrial geomorphological studies
325 Bentley et al (2007) describe the series of prominent inset lateral moraines that
326 document the recession of a fjord-based glacier along the south shore of Husvik Bay.
327 The most extensive of these (Bentley et al's. Limit I) was mapped on both sides of the
328 bay with further retreat positions marked by limits II and III and glacially abraded
329 bedrock (see Appendix Fig. A3, parts A and B). Submarine evidence of the extensive
330 Limit I retreat position appears to be evident in close inspection of the detailed
331 bathymetry of the bay (Fig. 6D and Appendix Fig. A3, parts A and B), but its subtle
332 sea-floor expression suggests that the inner basin retreat moraines have been at least
333 partially buried by high sediment flux from the former tidewater glaciers, and perhaps
334 more recently by inflowing sediment-laden rivers. The landward extent of our
335 multibeam dataset also hints at resolving the sea-floor expression of retreat Limit III
336 (Fig 6A), but not Limit II. The three lateral or frontal moraines mapped at the sea bed
337 between the tip of Berntson Ridge and Grass Island may correlate with the three
338 retreat limits (I-III) recorded by Bentley et al. (2007) in Husvik Harbour. This
339 interpretation would only be possible if the moraines were derived from the

340 Stromness Valley glacier rather than having formed at the juncture of the Leith and
341 Stromness valley glaciers, which would suggest a more complex glacial history.
342 Seaward of the inner basins and inner basin moraines the fjords merge into two
343 apparently distinct deeper basins, with noticeably different water depths (marked X
344 and Y on Fig 6A), that extend to the mouth of the fjord where there is a deep basin
345 moraine east of Framnaes Point (Fig. 6B), whose crest appears to lie deeper on the
346 Stromness (N) side of the merged fjord. Although they share a similar limit, these
347 may be two separate moraines. The difference in their ridge height probably reflects
348 the separation of basins in this part of the fjord and the formation of moraines by
349 individual glaciers. While bathymetry does deepen seaward offshore from the deep
350 basin moraine, unlike the other fjords, the outlet of Stromness Bay and Husvik Bay
351 does not obviously feed into a cross-shelf trough (Fig. 1).

352

353 3.5 Antarctic Bay

354 Antarctic Bay is a steep sided fjord, formed by the Crean Glacier, which remains a
355 significant tidewater outlet today (Fig. 7). The fjord is 8.5 km long and 2-2.5 km
356 wide, extending past Morse Point into one of the glacial troughs on the continental
357 shelf. Although bathymetric coverage is low, the data suggest the presence of a
358 shallow (30-150m deep) inner basin terminating in a moraine complex, comprising at
359 least three arcuate ice-marginal limits, seaward of which there is a deeper (200 m)
360 outer basin (Fig. 7B, 7C). These limits are more or less consistent with terrestrial
361 moraines on the west coast of the bay (Appendix Fig A4) that mark an expanded
362 position of the glaciers in the fjord but which have not yet been dated (Bentley et al.,
363 2007). The inner basin floor behind the three moraines is characterised by at least two
364 elongated ridges, one of which appears slightly sinuous (Fig 7A). These may have

365 been streamlined directly by the flow of grounded ice, or else comprise eskers
366 recording phases of meltwater deposition in subglacial tunnels near to the ice margin.

367

368 3.6 Possession Bay

369 Possession Bay is the outlet for the Purvis Glacier and a number of other tidewater
370 glaciers and ice fields (Fig. 8). The fjord is ~8 km long and up to 4 km wide (Fig.
371 7A). It has a relatively shallow inner basin terminating in a prominent moraine which
372 is visible at low tide (Fig. 8C, 8D). The moraine sits in a very similar fjord position to
373 the inner basin moraine mapped in the adjacent Antarctic Bay; marked 'outer moraine
374 reef' on Admiralty Chart 3585 (Harbours and Anchorages in South Georgia). The
375 inner basin moraine is consistent with a mapped position of a suite of onshore
376 moraines on the south east shore of Possession Bay (Bentley et al., 2007, Appendix
377 Fig. A5). The inner basin also exhibits a number of smaller retreat moraines (marked
378 with arrows) that record ice retreat to modern glacial extents (Fig. 8C). Beyond the
379 inner basin is a ~4 km-diameter, 350 m deep basin bounded on its northern side by a
380 60 m high, relatively well-preserved arcuate deep basin moraine (Fig. 8A, 8B),
381 situated 2 km north east of Black Head. Several lateral moraines are found farther
382 north still of the deep basin moraine, interpreted to have formed as medial features
383 between ice flowing out of Prince Olav Harbour and Possession Bay itself (Fig. 8A).

384

385 3.7 King Haakon Bay

386 King Haakon Bay was the only fjord surveyed on the south coast of South Georgia in
387 this study. It is one of the narrowest and longest fjords, being ~13 km long, up to ~3
388 km wide and relatively shallow at up to 160 m deep (Fig. 9). It is the outlet for the
389 Briggs Glacier, a major tidewater glacier which discharges from the east (Fig. 9A),

390 and a number of smaller tributary glaciers. The bathymetry data show a shallow inner
391 basin terminating in a 50-110 m high moraine, followed by a deeper basin offshore.
392 The deep basin bifurcates seaward around McCarthy Island, and shallows to 40-50 m
393 to the south. Linear features behind the moraine in the inner basin are evidence of
394 medial moraines or streamlined subglacially-formed ridges which may be analogous
395 to the medial moraine previously described from behind Husvik whaling station in
396 Husvik Bay; part of the same sequence that forms the Husvik Bay inner basin moraine
397 (Figs. 9A, 9B) (Limit III, Bentley et al., 2007). A number of smaller, minor arcuate
398 moraines, probably formed during recent phases of readvance or retreat, mark the
399 innermost 3 km of the basin where the fjord narrows towards the glacier front (Figs
400 9A, 9C).

401

402 3.8 Drygalski Fjord

403 Drygalski Fjord is the only major inlet at the south-eastern extremity of South
404 Georgia (Fig. 10). Like King Haakon Bay it is narrow and long, extending ~12 km
405 from the entrance at Natriss Head to the tidewater termini of the Risting and Jenkins
406 Glaciers. The fjord is 1-3 km wide (mostly <2 km), with a maximum depth of 220 m.
407 A number of tributary glaciers feed the fjord. The bathymetry survey reveals a large
408 shallower inner basin with a sinuously carved, flat-bottomed floor. Notably, the
409 deepest part of the basin extends to the present-day front of the Risting Glacier,
410 whereas the tributary connecting the fjord to Jenkins Glacier is surprisingly shallow,
411 suggesting that the Risting Glacier has been the dominant erosional system in the
412 fjord's evolution. A marked inner basin moraine connects to the headland west of the
413 entrance to Larsen Harbour, forming a pronounced loop marking a former ice-
414 marginal limit at the fjord mouth. Erosional grooves, probably subglacial in origin,

415 characterise the backslope of the moraine (Fig. 10B, black arrows), which has a
416 ‘wedge’-like asymmetric profile similar to that of the inner basin moraines in
417 Cumberland Bay East and West (Fig. 10C). This is one of the largest fjord moraines
418 in South Georgia. Beyond the moraine, the fjord bathymetry deepens to a <310-m
419 deep basin that extends south east and merges into a south westward trending cross-
420 shelf trough terminating in a deep basin moraine (see Fig 1 for its location). At least
421 three smaller moraines are observed stretching laterally across the innermost part of
422 the fjord, recording recent advance or retreat limits of the Risting and Jenkins Glaciers
423 (black arrows, Fig. 10A). Admiralty Chart 3585 (Harbours and Anchorages in South
424 Georgia) shows that Larsen Harbour has its own shallow inner basin terminating in a
425 moraine, marked Fairway Rock, and a series of possible truncated moraines before it
426 meets Drygalski Fjord.

427

428

429 **4. Discussion**

430

431 Despite the different lengths, widths and orientations of the fjords surveyed, a
432 relatively consistent pattern of large scale submarine geomorphological features has
433 emerged (Table 1). In particular, the majority of the fjords have a shallow inner basin
434 bounded by an inner basin moraine, a marked drop seaward into a deep basin with a
435 corresponding deep basin moraine at the outer limits of the fjord. Some fjords have
436 evidence of truncated moraines along the flanks of the deep basins. The outlets of all
437 the fjords are aligned with cross-shelf troughs (Fig. 1), with the exception of Husvik
438 and Stromness Bays. Most fjords are U- shaped with steep valley sides.

439

440 4.1 Relative ages of the glacial geomorphological features

441 Using a combination of previously published terrestrial radiocarbon, and cosmogenic
442 isotope exposure age constraints, together with the stratigraphic relationships between
443 the geomorphological features it is possible to reconstruct a relative glacial
444 chronology (Table 1; Fig. 11). According to analyses of the terrestrial glacial
445 geomorphology Clapperton (1971) and Bentley et al. (2007) found that all moraines
446 in the Stromness Bay and Cumberland Bay East and West are confined to the inner
447 fjords, whilst the outer headlands are devoid of major onshore depositional landforms.
448 In Cumberland Bay East, Antarctic Bay and possibly Possession Bay the most
449 seaward of the terrestrial moraines mapped by Bentley et al. (2007) coincide with the
450 position of the submarine inner fjord moraines (Appendix Figs. A1, A4, A5). Bentley
451 et al (2007) attempted to date this feature in Cumberland Bay East at Moraine Fjord
452 (Fig. 4 and Appendix Fig. A1), but the ^{10}Be age had an unacceptably large error
453 (GRE5, $12,900 \pm 7800$). These inner basin moraines have a cross section that, in
454 comparison with conceptual models of tidewater glacier sedimentation (Powell, 2003,
455 Figs. 13.7 & 13.17) suggests they are push moraine banks formed at an advancing
456 grounding line. Their characteristics including profile asymmetry, generally rounded
457 crests, as well as evidence, in some examples, of thrust-blocks within the moraine belt
458 (e.g. Fig. 2), are all diagnostic of bull-dozed moraine banks. In combination with their
459 size, at 10s of metres high, the moraines are therefore taken as indicators of a
460 maximum grounding line advance rather than moraines formed during retreat from an
461 otherwise more expansive glacial extent. Given the preservation of these features, it is
462 high unlikely that these moraines have been overridden since their formation because
463 any subsequent advance would have presumably cannibalised any existing sediment
464 bodies. Glacial retreat in the inner basins has likely been accompanied by large

465 volumes of glacimarine sediment deposition which has accumulated behind the inner
466 moraine contributing to inner basin moraine profiles that have an asymmetric
467 morphology rising gradually 20-100 m to a moraine crest then descending steeply 30-
468 160 m into the deep basin on the seaward side. The difference between the depth of
469 the shallow inner, and deep outer basins can therefore be attributed to a high sediment
470 flux between the glacier termini and the inner basin moraines, coupled with rapidly
471 shallowing underlying basement rocks. In those surveys with exceptional sea-floor
472 detail (e.g. Royal Bay, Cumberland Bay East) these accumulations of inner-basin
473 sediments are characterised by a range of sedimentary features including sediment
474 gravity flows, debris fans and slope failures, all of which can be associated with high
475 sediment supply. At some sites (e.g. Royal Bay) the inner moraines may have been
476 partially breached and subsequent debris flows have created debris fans which overlie
477 older glacial deposits. However in general debris fans are absent from the deep basins
478 with the exception of sites where tributary glaciers discharge into the fjords, for
479 example where Moraine Fjord and the Hamberg Valley discharge into Cumberland
480 Bay East.

481

482 The large volume of glacial sediments in the inner basins appears to have, in some
483 cases, buried any evidence of retreat moraines in the inner basins, and these latter
484 features appear to be better preserved on land for example in Husvik Bay and
485 Cumberland West Bay (Clapperton et al., 1989; Bentley et al., 2007) (Appendix Figs.
486 A2,A3). Some potential evidence of inner basin retreat moraines however was found
487 in Cumberland Bay East (Fig. 4), as well as in the innermost parts of Husvik Bay,
488 Antarctic Bay, Possession Bay, King Haakon Bay, and Drygalski Fjord. The
489 terrestrial moraines in these inner basin regions are interpreted as marking the oldest

490 mapped ice advance on South Georgia and have cosmogenic ^{10}Be exposure ages of
491 between 14.2 and 10.6 ka BP, mean 12.2 ± 1.5 ka BP, based on data from the Husvik
492 medial moraine (Bentley et al., 2007, 'category a' moraines) (Appendix Fig. A3).
493 These 'category a' moraines have been correlated on geomorphological grounds with
494 the oldest terrestrial moraine ridges in Antarctic Bay, Possession Bay and Moraine
495 Fjord (Zenker Ridge) (Appendix Figs. A4, A5, A1, respectively). If these dates are
496 correct, this suggests that glacier retreat from the inner basin moraine took place
497 during the warming that followed the Antarctic Cold Reversal; the abrupt cooling in
498 Antarctica which occurred between 14,540 and 12,760 years ago and is associated
499 with glacier expansions as far north as 44° S (Putnam et al., 2010). Landward of these
500 moraines is a second set of moraines documenting a mid-Holocene advance at $3600 \pm$
501 1100 yr BP (Bentley et al., 2007, 'category b' moraines) (Appendix Fig. A1). In some
502 areas this advance approached nearly to the 'category a' limits. If the LGM on South
503 Georgia was restricted to the inner fjords, as suggested by Bentley et al. (2007) then
504 the inner basin fjord moraines would represent the maximum grounding lines (Fig.
505 11). The asymmetry between the position of the inner basin moraines in Husvik and
506 Stromness Bays (Fig. 6 and Appendix Fig. A3) would place Tonsberg Point in a
507 favourable position to avoid overriding glacial ice and may explain why 18.6 ka lake
508 sediments are found there (Rosqvist et al., 1999; Rosqvist and Schuber, 2003).
509
510 We rule out a Little Ice Age (LIA) date for the inner basin moraines because this
511 would be inconsistent with the available cosmogenic and radiocarbon age constraints.
512 In addition the LIA, or at least the most recent advance, has been shown as a
513 relatively minor advance of the higher mountain glaciers (Clapperton, 1971; Roberts
514 et al., 2010). In Royal Bay, Gordon and Timmins (1992) also interpreted very minor

515 readvance of the Ross Glacier during the LIA, based on the presence of heavily
516 vegetated shore-side moraines, which lie just beyond the 20th Century glacier limit.
517

518 All the fjords in this study have a deep basin, a majority have a deep basin moraine
519 and between 5 and 7 have features which might be interpreted as truncated moraines
520 along the flanks of the deep basin, because they apparently do not have a bedrock
521 control (Fig. 11). Deep basin moraines can also be seen in other fjords not surveyed in
522 this study, such as the major submarine fjord which discharges from the west side of
523 the Bay of Isles (Fig. 1, circled). There is little evidence of events coinciding with the
524 formation of the deep basin moraines being preserved on land. Instead the coastal
525 areas adjacent to the deep basin moraines contain only patchy degraded till veneers
526 and a very limited number of glacial erratics of unknown age (Bentley et al., 2007).
527 Based on this weathering and a proposed morphological distinction between last
528 glaciation and older landforms (Bentley et al., 2007), our interpretation is that the
529 deep basin moraine may represent an older pre-LGM glaciation; the simplest
530 interpretation being that it is the penultimate MIS6 glacial limit in the fjords (Fig. 11).
531 Where it is well preserved, it shares a similar cross-section to the inner basin moraine,
532 with an asymmetric morphology rising gradually 25-60 m to a moraine crest then
533 descending steeply 40-90 m on the seaward side. Good examples of this are found at
534 the mouth of Cumberland Bay East and Possession Bay and similar features have
535 been described from the southern Chilean fjords (Fig. 7B in Dowdeswell and
536 Vásquez, 2013). Not all are well preserved, for example in Cumberland West Bay the
537 moraine is breached on its eastern side, possibly by iceberg scouring or a readvance of
538 the combined Neumayer, Geikie and Lyell Glaciers, although the latter is less likely
539 as it should have removed the entire moraine, at least in the central part of the fjord.

540

541 Features inferred to be truncated moraines, where present, are usually located along
542 the sides of the deep basins (Fig. 11). These are interpreted as recording a series of
543 successive glacial advances that pre-date the deep basin moraine. Seaward of the deep
544 basin moraine most of the fjords merge with 250-380 m deep cross shelf troughs that
545 vary between 40-102 km in length and 2-5 km wide in the inner shelf to 12-26 km
546 wide on the middle and outer shelf (Graham et al., 2008) (Fig. 1). These also have
547 broadly similar cross sections to those seen in the fjords, in particular several mid-
548 trough moraines (Fig 5a in Graham et al., 2008) which mark the position of one
549 glacial advance, and more distal moraines and at least one trough mouth fan on the
550 shelf edge which mark a series of older and maximum glaciation(s). However,
551 because of the less well defined and rounded nature of many of these moraines our
552 interpretation is that the outer parts of these troughs were not ice-filled at the LGM,
553 and instead moraines mark a series of older glaciation(s). The troughs themselves are
554 likely to have formed since the Late Miocene and thus glaciations may be as old as
555 the early Pleistocene, and more similar to those seen off the coast of Patagonia
556 (Rabassa, 2000; Singer et al., 2004). Older terrestrial rock platforms e.g. at c. 21 m in
557 Harpon Bay and 24 m in Carlita Bay (Bentley et al., 2007, p.655), that are overprinted
558 by later moraines may reflect the glacioisostatic depression from these continental
559 shelf glaciations. Similar altitude terrestrial rock platforms have been observed
560 elsewhere between 2-3.5 and 5.5-7.5 m above sea level (Adie, 1964; Stone, 1974).

561

562 The apparent absence of glacial lineations, streamlined bedforms, drumlins and other
563 flow-parallel features in the fjords, as found for example in Marguerite Bay (Ó
564 Cofaigh et al., 2005) on the Antarctic Peninsula, some of the Southern Chilean fjords

565 (Dowdeswell and Vásquez, 2013) and at the mouth of the Kongsfjorden-Krossfjorden
566 system in Svalbard (MacLachlan et al., 2010), suggests that the features have been
567 buried by post-glacial sedimentation via turbid meltwater plumes from glaciers and
568 sediment delivery from icebergs which can discharge high volumes of sediment into
569 the fjord environment. In a previous study, Graham et al. (2008) showed evidence for
570 drumlinised topography on part of the South Georgia continental shelf where
571 sediments presumably thin out or are absent. Furthermore, towards the mouths of the
572 fjords in both Drygalski Fjord and King Hakkon Bay there is some indication in the
573 bathymetry that exposed bedrock or basin sediments have been streamlined by past
574 ice flow, while large moraines attest to significant delivery of subglacial sediment.
575 Thus, while there is no clear evidence for full ice-stream style drainage, it remains
576 possible that several or more glaciers that drained the former South Georgia ice cap
577 were fast-flowing, and actively eroded and modified their bed.

578

579 4.2 Regional significance

580 Collectively the data presented here suggest that LGM was limited to the inner fjords
581 as implied by Bentley et al. (2007) . This might imply a degree of sea level control on
582 glacier extent, with the lower LGM sea level resulting in some of the glacier fronts
583 being grounded on land within the inner basins. This is supported by studies of recent
584 glacial retreat in Greenland which has shown that marine-terminating outlet glaciers
585 have thinned more rapidly than land-terminating outlet glaciers (Sole et al., 2008).
586 Thus in situations where the glaciers were grounded on land they may not have
587 advanced beyond the inner basin moraines.

588

589 Another factor resulting in the limited glacial extent at the LGM could be that the
590 glaciers were deprived of moisture by the more extensive sea ice during the later
591 stages of the last glacial (Allen et al., 2011; Collins et al., 2012). This is a common
592 feature of sub-Antarctic islands where the combination of sea ice further north and
593 strong winds increased aridity (Hodgson et al., 0000; Bentley et al., 2007) – hence
594 most peat and lake sequences in the sub-Antarctic region only start to accumulate in
595 the early to mid-Holocene (Van de Putten and Verbruggen, 2005; Van de Putten,
596 2008), with occasional exceptions between 19000 cal yr BP and the start of the
597 Holocene (Selkirk et al., 1988; Keenan 1995; Rosqvist et al., 1999). Patagonian
598 climate, east of the Andes was also arid at this time (Recasens et al., 2011) due, in
599 part to the same factors, together with the rain shadow effect of the mountains.

600

601 In addition to changes in sea ice extent, reduced moisture delivery is a product of a
602 northward shift of the Southern Hemisphere westerly winds. One simplified study
603 with a general circulation model (Toggweiler et al., 2006) suggests that the belt of the
604 Southern Hemisphere westerly winds may move northward towards the Equator
605 during cold periods (and vice versa). This would suggest that moisture supply seems
606 to be a major factor in the mass balance of the South Georgia glaciers (Bentley et al.,
607 2007; Gordon et al., 2008), with insolation and aspect being of lesser importance.

608 Unravelling the sequence and extent of South Georgia (and other subantarctic)
609 glaciations could therefore provide important information on long term changes in the
610 position of the Southern Hemisphere Westerlies (moisture supply from subtropical air
611 masses) and changes in glacial sea ice extent (aridity).

612

613 An alternative hypothesis is that over many glacial cycles, the glacial erosion of the
614 alpine valleys and fjords has been sufficient to reduce the length of glaciers in the
615 most recent cycle because theoretically glacier length can scale linearly with erosion
616 depth (Anderson et al. 2012). In such cases there are often earlier moraines deposited
617 well beyond the LGM limits. These are referred to by Anderson et al. (2012) as ‘far-
618 flung’ moraines. This suggests that the glacially modified landscape, rather than a
619 different climate, may be capable of explaining at least some of the earlier more
620 extensive glacier extents, but this hypotheses has yet to be tested in detail..

621

622 Biological studies of the South Georgia continental shelf have shown that it is a
623 hotspot for biodiversity; a possible result of it being an ice free refuge for the biota
624 through several glacial cycles (Barnes et al., 2011; Hogg et al., 2011). Terrestrial
625 glacial refuges were also present for endemic birds on the island with molecular
626 biological data pointing to divergence of the South Georgia Pintail (*Anas georgica*
627 *georgica*) from the neighbouring Argentinian population of yellow-billed pintails (*A.*
628 *georgica spinicauda*) prior to the Last Glacial Maximum (McCracken et al. 2013).
629 Therefore better dating of the shelf sediments and geomorphological features will
630 provide a temporal context to the emerging evolutionary history of the Antarctic and
631 Southern Ocean biota. Thus, the need for a robust glacial chronology extends beyond
632 fields of geoscience and palaeoclimate studies.

633

634

635 4.3 Future work

636 South Georgia’s location at the heart of the Southern Ocean, means that the phase
637 relationships, forcing, and magnitude of glacial events on the island and its adjoining
638 shelf are likely to provide crucial insights into how climate has fluctuated through

639 time, enabling correlation of records regionally (to South America and the Antarctic
640 Peninsula), and with climatic and ice sheet variability at the global scale. Therefore it
641 is important to do further work to establish whether the South Georgia glaciers were
642 indeed grounded in their inner fjords at the LGM (Bentley et al., 2007), or extended
643 onto the continental shelf, or indeed reached the continental shelf break (Graham et
644 al., 2008). In order to determine this, sampling of sediments either side of the inner
645 basin, deep basin and mid-shelf moraines is required. Specifically, by dating the
646 sediments and showing that they are glacimarine or fully open marine would provide
647 a minimum constraint on deglaciation, and dating material within or below tills would
648 provide maximum constraints. TOPAS (0.5-5 kHz) sub-bottom profiler data from
649 Cumberland Bay shows cross-sections of the outer basin moraine as well as the deep
650 basin landward of this feature (Fig. 4E). Both features are draped with sediments. The
651 chaotic unit at the base of the outer basin has an acoustic signature that is normally
652 associated with diamicton, such as glacial till, but it is not present, or not resolved, in
653 sedimentary basins on the seaward side of the moraine. Sediment coring will help
654 define whether this unit is indeed the LGM till. This hypothesis will be tested in
655 future work that will also involve dating the glacial sequence beyond the outer
656 moraines.

657

658 Further shallow water seismic surveys (e.g. Fig 4E) would also be advantageous to
659 map the basic depositional architecture of the sediment facies within these moraines
660 and to compare them with sedimentological models (e.g. Fig. 13.17 in Powell, 2003)
661 and terrestrial evidence. Previous studies in sub-polar and polar fjords have found that
662 sediment can be preserved from several glacial episodes (Barrett and Hambrey, 1992)
663 and studies of Antarctic Peninsula Fjords have shown the presence of distinct

664 interglacial sequences comprising diatomaceous sediments in spring and summer and
665 an enhanced terrigenous sediment supply in winter (Allen et al., 2010). If this is the
666 case at South Georgia then it may be possible to reconstruct the limits of several
667 previous glaciations and glacial advances. For the oldest glaciations the relative
668 chronology could be established by extracting marine sediment cores from the trough
669 mouth fans at the end of the cross shelf troughs and farther down the slope on
670 sediment drift bodies. The potential of the former features has been previously
671 recognised (Graham et al., 2008). The conclusion of Clapperton and Sugden (1988),
672 that ‘much of the evidence on which the chronology of glacier fluctuations in South
673 America and Antarctica is based appears to be tenuous and, in places, highly
674 ambiguous’ still applies to South Georgia today but could be rapidly addressed by a
675 marine geological coring programme.

676

677

678 **5. Conclusions**

679

680 Mapping of the submarine geomorphology in nine of South Georgia’s innermost
681 fjords has revealed a relatively consistent pattern of submarine geomorphological
682 features. These include a shallow inner basin bounded by an inner basin moraine, a
683 deep basin, and a deep basin moraine at the outer limits of the fjords. Some fjords
684 have evidence of truncated moraines in the deep basins. The outlets of all the fjords
685 were aligned with cross-shelf troughs, with the exception of Husvik and Stromness
686 Bays.

687

688 A relative chronology based on existing terrestrial evidence suggests that the inner
689 basin moraines date from the last major glacial advance (LGM), and the deep basin
690 moraines from an earlier glaciation, possibly MIS 6. On the sides of the deep basin
691 trough a series of truncated moraines show ice advance positions from preceding
692 periods. Based on the existing chronological constraints the cross shelf troughs, and
693 mid-trough moraines are interpreted as the product of glaciations that pre-date the
694 LGM.

695

696 LGM glaciers persisted until the end of the Antarctic Cold Reversal and then retreated
697 during the Holocene, punctuated by a series of readvances towards the LGM limit (cf.
698 Clapperton, 1971; Bentley et al., 2007).

699

700 If correct, the relative stratigraphic relationships between the various
701 geomorphological features and previously published age constraints suggest that the
702 glacial history of South Georgia is more similar to that of Southernmost South
703 America where a series of Pleistocene glaciations (of MIS 20 and younger) extended
704 beyond LGM limits in Patagonia (Rabassa, 2000; Coronato et al., 2004), with the
705 most extensive glacial advance occurring *c.* 1.1 Ma (Singer et al., 2004). Further
706 marine geological records are required to test this interpretation.

707

708

709 **Acknowledgements**

710

711 The data used in this study are derived from swath bathymetric surveys carried out by
712 HMS *Endurance* in 2005 and 2006, together with data from the British Antarctic

713 Survey RRS *James Clark Ross*. Captain Nick Lambert of HMS *Endurance*, the
714 surveyors George Tabart and Ken Smith and the BAS staff are thanked for their
715 enthusiasm for completing the surveys under, sometimes, challenging conditions.
716 Tara Deen and Alex Tait (BAS) are thanked for their help with archiving and
717 accessing the data. AGCG is supported by Natural Environment Research Council
718 (NERC) New Investigator Grant, NEK0005271. We thanks our reviewers for their
719 constructive comments.

720

721

722

723 **References**

- 724 Adie, R.J., 1964. Sea-level changes in the Scotia arc and Graham Land. In: R.J. Adie
725 (Editor), *Antarctic Geology*. North-Holland Publishing Company, Amsterdam,
726 pp. 27-32.
- 727 Allen, C.S., Oakes-Fretwell, L., Anderson, J.B. and Hodgson, D.A., 2010. A record of
728 Holocene glacial and oceanographic variability in Neny Fjord, Antarctic
729 Peninsula. *The Holocene* 20(4), 551–564.
- 730 Allen, C.S., Pike, J. and Pudsey, C.J., 2011. Last glacial-interglacial sea-ice cover in
731 the SW Atlantic and its potential role in global deglaciation. *Quaternary*
732 *Science Reviews* 30(19-20), 2446-2458.
- 733 Anderson, R.S., Dühnforth, M., Colgan, W., and Anderson, L., 2012 Far-flung
734 moraines: Exploring the feedback of glacial erosion on the evolution of glacier
735 length. *Geomorphology* 179, 269-285.
- 736 Barnes, D.K.A., Collins, M.A., Brickle, P. and Fretwell, P., 2011. The need to
737 implement the Convention on Biological Diversity at the high latitude site,
738 South Georgia. *Antarctic Science* 23(4), 323-331,
739 doi:10.1017/S0954102011000253.
- 740 Barrett, P.J. and Hambrey, M.J., 1992. Plio-Pleistocene sedimentation in Ferrar Fjord,
741 Antarctica *Sedimentology* 39, 109-123.
- 742 Bentley, M.J., Evans, D.J.A., Fogwill, C.J., Hansom, J.D., Sugden, D.E. and Kubik,
743 P.W., 2007. Glacial geomorphology and chronology of deglaciation, South
744 Georgia, sub-Antarctic. *Quaternary Science Reviews* 26(5-6), 644-677.
- 745 Broecker, W.S., 1998. Paleocean circulation during the last deglaciation: a bi-polar
746 seesaw? *Paleoceanography* 13, 119-121.

747 Clapperton, C.M., 1971. Geomorphology of the Stromness Bay-Cumberland Bay
748 area, South Georgia. *British Antarctic Survey Scientific Reports* 70.

749 Clapperton, C.M. and Sugden, D.E., 1988. Holocene glacier fluctuations in South
750 America and Antarctica. *Quaternary Science Reviews* 7, 185-198.

751 Clapperton, C.M., Sugden, D.E., Birnie, J. and Wilson, M.J., 1989. Later-Glacial and
752 Holocene glacier fluctuations and environmental change on South Georgia,
753 Southern Ocean. *Quaternary Research* 31, 210-228.

754 Collins, L.G., Pike, J., Allen, C.S. and Hodgson, D.A., 2012. High resolution
755 reconstruction of southwest Atlantic sea-ice and its role in the carbon cycle
756 during marine isotope stages 3 and 2. *Palaeoceanography* 27, PA3217,
757 doi:10.1029/2011PA002264.

758 Cook, A.J., Poncet, S., Cooper, A.P.R., Herbert, D.J. and Christie, D., 2010. Glacier
759 retreat on South Georgia and implications for the spread of rats. *Antarctic
760 Science* 22(3), 255-263.

761 Coronato, A., Martínez, M.A. and Rabassa, J., 2004. Glaciations in Argentine
762 Patagonia, southern South America. In: J. Ehlers and P.L. Gibbard (Editors),
763 *Quaternary Glaciations - Extent and Chronology, Part III*. Elsevier, pp. 49-67.

764 Dowdeswell, J.A. and Vásquez, M., 2013. Submarine landforms in the fjords of
765 southern Chile: implications for glacial-marine processes and sedimentation in a
766 mild glacier-influenced environment. *Quaternary Science Reviews* 64, 1-19.

767 Fretwell, P.T., Tate, A.J., Deen, T.J. and Belchier, M., 2009. Compilation of a new
768 bathymetric dataset of South Georgia. *Antarctic Science* 21(2), 171-174.

769 Gordon, J.E., 1987. Radiocarbon dates from Nordenskjöld Glacier, South Georgia,
770 and their implications for late Holocene glacier chronology. *British Antarctic
771 Survey Bulletin* 76, 1-5.

772 Gordon, J.E. and Timmis, R.J., 1992. Glacier fluctuations on South Georgia during
773 the 1970s and early 1980s. *Antarctic Science* 4(2), 215–226.

774 Gordon, J.E., Haynes, V.M. and Hubbard, A., 2008. Recent glacier changes and
775 climate trends on South Georgia. *Global and Planetary Change* 60(1-2), 72-84.

776 Graham, A.G.C., Fretwell, P.T., Larter, R.D., Hodgson, D.A., Wilson, C.K., Tate,
777 A.J. and Morris, P., 2008. New bathymetric compilation highlights extensive
778 paleo-ice sheet drainage on the continental shelf, South Georgia, sub-
779 Antarctica. *Geochemistry Geophysics Geosystems* in press.

780 Gregory, J.W., 1915. The physiography of South Georgia as shown by Mr Ferguson's
781 photographs. In: D. Ferguson (Editor), *Geological observations in South*
782 *Georgia*. Transactions of the Royal Society of Edinburgh, Vol. 50, Part 4, pp.
783 814-816.

784 Hodgson, D.A., Graham, A.C.G., Roberts, S.J., Bentley, M.J., ÓCofaigh, C.,
785 Verleyen, E., Jomelli, V., Favier, V., Brunstein, D., Verfaillie, D., Colhoun,
786 E.A., Saunders, K., Mackintosh, A., Hall, K., McGlone, M.S. and Van der
787 Putten, N., 0000. Terrestrial and marine evidence for the extent and timing of
788 glaciation on the sub-Antarctic islands. *Quaternary Science Reviews*.

789 Hogg, O.T., Barnes, D.K.A. and Griffiths, H.J., 2011. Highly Diverse, Poorly Studied
790 and Uniquely Threatened by Climate Change: An Assessment of Marine
791 Biodiversity on South Georgia's Continental Shelf. *PLoS ONE* 6(5), e19795.

792 Howe, J.A., Austin, W.E.N., Forwick, M. and Paetzel, M., 2010. *Fjord Systems and*
793 *Archives*. Geological Society, London, Special Publications 344, 380pp.

794 Keenan, H., 1995. *Modern and Fossil Terrestrial and Freshwater Habitats on*
795 *Subantarctic Macquarie Island*, Macquarie University.

796 MacLachlan, S.E., Howe, J.A. and Vardy, M.E., 2010. Morphodynamic evolution of
797 Kongsfjorden-Krossfjorden, Svalbard, during the Late Weichselian and
798 Holocene. In: J.A. Howe, W.E.N. Austin, M. Forwick and M. Paetzel
799 (Editors), Fjord Systems and Archives. Geological Society of London, Special
800 Publications pp. 195-205.

801 McCracken, K.G., Wilson, R.E., Peters, J.L., Winker, K. and Martin, A.R., 2013. Late
802 Pleistocene colonization of South Georgia by yellow-billed pintails pre-dates
803 the Last Glacial Maximum. *Journal of Biogeography*. Published online: 26
804 JUN 2013, DOI: 10.1111/jbi.12162.

805 Ó Cofaigh, C. and J.A., D., 2001. Laminated sediments in glacimarine environments:
806 diagnostic criteria for their interpretation. *Quaternary Science Reviews* 20,
807 1411-1436.

808 Ó Cofaigh, C., Dowdeswell, J.A., Allen, C.S., Hiemstra, J.F., Pudsey, C.J., Evans, J.
809 and Evans, D.J.A., 2005. Flow dynamics and till genesis associated with a
810 marine-based Antarctic palaeo-ice stream. *Quaternary Science Reviews* 24,
811 709-740.

812 Pfirman, S.L. and Solheim, A., 1989. Subglacial meltwater discharge in the open-
813 marine tidewater glacier environment: observations from Nordaustlandet,
814 Svalbard archipelago. *Marine Geology* 86, 265-281.

815 Powell, R.D. and Alley, R.B., 1997. Grounding line systems: processes, glaciological
816 inferences and the stratigraphic record. In: P.F. Barker and A.C. Cooper
817 (Editors), *Geology and seismic stratigraphy of the Antarctic margin*, 2.
818 Antarctic Research Series 7, AGU Washington DC, pp. 169-187.

819 Powell, R.D., 2003. Subaquatic Landsystems: Fjords. In: D.J.A. Evans (Editor),
820 *Glacial Landsystems*. Arnold, London, pp. 313-347.

821 Putnam, A.E., Denton, G.H., Schaefer, J.M., Barrell, D.J.A., Andersen, B.G., Finkel,
822 R., Schwartz, R., Doughty, A.M., Kaplan, M.R. and Schlüchter, C., 2010. The
823 atmospheric footprint of the Antarctic Cold Reversal in southern middle
824 latitudes. *Nature Geoscience* 3 700-704.

825 Rabassa, J., 2000. Quaternary of Tierra del Fuego, southernmost South America: An
826 updated review. *Quaternary International* 68-71, 217-240.

827 Recasens, C., Ariztegui, D., Gebhardt, C., Gogorza, C., Haberzettl, T., Hahn, A.,
828 Kliem, P., Lisé-Pronovost, A., Lücke, A., Maidana, N.I., Mayr, C., Ohlendorf,
829 C., Schäbitz, F., St-Onge, G., Wille, M., Zolitschka, B. and ScienceTeam, P.,
830 2011. New insights into paleoenvironmental changes in Laguna Potrok Aike,
831 Southern Patagonia, since the Late Pleistocene: the PASADO multiproxy
832 record. *The Holocene* 0959683611429833.

833 Roberts, S.J., Hodgson, D.A., Shelley, S., Royles, J., Griffiths, H.J., Thorne, M.A.S.
834 and Deen, T.J., 2010. Establishing age constraints for 19th and 20th century
835 glacier fluctuations on South Georgia (South Atlantic) using lichenometry.
836 *Geografiska Annaler (A)* 92A(1), 125-139.

837 Rosqvist, G.C., Rietti-Shati, M. and Shemesh, A., 1999. Late glacial to middle
838 Holocene climatic record of lacustrine biogenic silica oxygen isotopes from a
839 Southern Ocean island. *Geology* 27(11), 967-970.

840 Rosqvist, G.C. and Schuber, P., 2003. Millennial-scale climate changes on South
841 Georgia, Southern Ocean. *Quaternary Research* 59, 470-475.

842 Selkirk, D.R., Selkirk, P.M., Bergstrom, D.M. and Adamson, D.A., 1988. Ridge top
843 peats and palaeolake deposits on MacQuarie Island. *Proceedings of the Royal*
844 *Society of Tasmania* 122(1), 83-90.

845 Singer, B.S., Ackert, R.P.J. and Guillou, H., 2004. $^{40}\text{Ar}/^{39}\text{Ar}$ and K-Ar chronology
846 of Pleistocene glaciations in Patagonia. Geological Society of America
847 Bulletin 116, 434-450.

848 Sole, A., Payne, T., Bamber, J., Nienow, P. and Krabill, W., 2008. Testing hypotheses
849 of the cause of peripheral thinning of the Greenland Ice Sheet: is land-
850 terminating ice thinning at anomalously high rates? *The Cryosphere* 2, 205-
851 218.

852 Stone, P., 1974. Physiography of the north-east coast of South Georgia. *British*
853 *Antarctic Survey Bulletin* 38, 17-36.

854 Sugden, D.E. and Clapperton, C.M., 1977. The maximum ice extent on island groups
855 in the Scotia Sea, Antarctica. *Quaternary Research* 7, 268-282.

856 Sugden, D.E., 2009. Ice sheets and ice caps. In: O. Slaymaner, T. Spencer and C.
857 Embleton-Hammann (Editors), *Geomorphology and global environmental*
858 *change*. Cambridge University Press, Cambridge.

859 Toggweiler, J.R., Russell, J.L. and Carson, S.R., 2006. Midlatitude westerlies,
860 atmospheric CO₂, and climate change during the ice ages. *Palaeoceanography*
861 21 PA2005, doi:10.1029/2005PA001154.

862 Van de Putten, N. and Verbruggen, C., 2005. The onset of deglaciation of
863 Cumberland Bay and Stromness Bay, South Georgia. *Antarctic Science* 17(1),
864 29-32.

865 Van de Putten, N., 2008. Post-glacial palaeoecology and palaeoclimatology in the
866 sub-Antarctic, University of Ghent, Ghent, 266 pp.

867 Van der Putten, N., Stieperaere, H., Verbruggen, C. and Ochyra, R., 2004. Holocene
868 palaeoecology and climate history of South Georgia (sub-Antarctic) based on
869 a macrofossil record of bryophytes and seeds. *The Holocene* 14(3), 382-392.

870 Van der Putten, N., 2008. Post-glacial palaeoecology and palaeoclimatology in the
871 sub-Antarctic, University of Ghent, Ghent, 266 pp.

872 Wasell, A., 1993. Diatom stratigraphy and evidence of environmental changes in
873 selected lake basins in the Antarctic and South Georgia. Report 23, Stockholm
874 University, Department of Quaternary Research, Stockholm.

875

876

877

878 **Table**

879

880 Table 1. Presence and number of key submarine glacial geomorphological features
881 identified in the South Georgia fjords from swath bathymetric and bathymetric
882 soundings. Age constraints for these features are based on a combination of terrestrial
883 age constraints (radiocarbon dates and cosmogenic isotope dating) and the relative
884 geochronological relationships between various terrestrial and submarine features (see
885 Appendix A figures). *located in the inner basin based on terrestrial evidence.

886 †circled on Fig. 1.

887

888

889 **Figure captions**

890

891 Figure 1A. Topographic and bathymetric compilation of South Georgia and its
892 continental shelf (223 m cell size grid, UTM Zone 24S projection) compiled from a
893 variety of data sources including, multibeam swath and single-beam bathymetry data
894 (Graham et al., 2008; Fretwell et al., 2009). Note the aligned trough systems widening
895 from the fjords towards the outer shelf, converging tributaries, banked shelf edge
896 features, well-defined shape of the continental margin, and radial distribution of
897 troughs north and south of the island. Hillshade of DEM of South Georgia supplied by
898 P. Fretwell, BAS. Locations of Figures 2-9 are shown as inset boxes. Circles highlight
899 the deep basins at Bay of Isles (northwest coast) and Drygalski Fjord (east coast).
900 Inset map shows the wider regional location of South Georgia with grey shading
901 indicating water depths <500m. Oceanographic boundaries indicated are the Polar

902 Front, the Sub-Antarctic Front (SAF) and the southern Antarctic Circumpolar Current
903 Front (SACCF).

904

905 Figure 1B. Oblique aerial photograph along the heavily glaciated south coast of South
906 Georgia facing west from near the head of Drygalski Fjord.

907

908 Figure 2. Multibeam swath bathymetry and geomorphological features of Royal Bay,
909 South Georgia. Inset boxes show (B) a cross section along the fjord, (C) an enlarged
910 image of the truncated ridges or moraines, (D) cross-section of the truncated ridges or
911 moraines (E) an enlarged image of the inner basin, and (F) an enlarged image of the
912 inner basin moraine.

913

914 Figure 3. Oblique perspective image of multibeam swath bathymetry from the inner
915 basin, Royal Bay, showing sea-floor geomorphic features including sets of small
916 ridges and an active or recently-active meltwater gully. Glacier flow, today, is
917 towards the reader. Image is approximately 3 km across in the forefield.

918

919 Figure 4. Multibeam swath bathymetry of Cumberland Bay East, South Georgia. HV:
920 Hamburg Valley; HS: Hestesletten; KEC: King Edward Cove. Inset boxes show (B)
921 an enlarged image of the inner basin and inner basin moraine, (C) an enlarged image
922 of the outer basin moraine, (D) a cross section along the fjord and (E) a TOPAS sub-
923 bottom profile collected on the RRS *James Clark Ross* cruise JR224 shows cross-
924 sections of both the outer deep basin moraine as well as the second remnant moraine
925 landward of this feature.

926

927 Figure 5. Multibeam swath bathymetry of Cumberland Bay West, South Georgia.

928 Inset boxes show (B) an enlarged image and (C) a cross section of the partially

929 preserved outer basin moraine, and (D) a cross section of the inner basin.

930

931 Figure 6 (upper panel). Multibeam swath bathymetry and geomorphological features

932 of Stromness and Husvik Bays, South Georgia. Inset boxes show (B) a cross section

933 of the inner basin moraine and (C) a cross section of the outer deep basin moraine.

934

935 Fig 6 (lower panel). Oblique aerial photograph of Husvik Bay and Tonsberg Point

936 facing approximately south west. HMS *Endurance* is present in Husvik Harbour (to

937 the right of the image) for scale.

938

939 Figure 7. Multibeam swath bathymetry and geomorphological features of Antarctic

940 Bay, South Georgia. Inset boxes show (B) an enlarged image and (C) cross-section of

941 the moraine complex at the seaward end of the inner basin, comprising at least three

942 ice-marginal limits.

943

944 Figure 8. Multibeam swath bathymetry and geomorphological features of Possession

945 Bay, South Georgia. Inset boxes show (B) an enlarged image of the deep basin

946 moraine, (C) an enlarged image of the inner basin moraine, and (D) a cross section of

947 the deep basin and deep basin moraine.

948

949 Figure 9. Multibeam swath bathymetry and geomorphological features of King

950 Haakon Bay, South Georgia. Inset boxes show (B) a transverse cross-section of the

951 medial moraines and (C) a cross section along the fjord.

952

953 Figure 10. Multibeam swath bathymetry and geomorphological features of Drygalski
954 Fjord, South Georgia. Inset boxes show (B) an enlarged image of the inner basin
955 moraine showing the erosional grooves that characterise the back slope of the moraine
956 (black arrows) and (C) a cross section of the inner basin moraine.

957

958 Figure 11. Cross-section schematic of a typical South Georgia glaciated fjord,
959 showing main geomorphic features, correlation to onshore chronological constraints,
960 and inferred ages from this study. In our model, features seaward of the deep basin
961 moraine on the continental shelf (not shown) are proposed as older than the
962 penultimate glacial episode, MIS6. ^a this study; ^b ages from terrestrial studies of
963 Bentley et al. (2007) and Rosqvist et al. (1999).

964

965 **Appendix A**

966 Appendix A contains figures showing the detailed submarine geomorphology of the
967 South Georgia fjords spliced together with the terrestrial glacial geomorphological
968 maps of Bentley et al. (2007), to illustrate the geomorphological and chronological
969 relationships between these datasets .

970

971 Appendix Figure A1. Multibeam swath bathymetry of Cumberland Bay East, South
972 Georgia combined with Figures 7a (west coastline); 7b (Szielasko Valley); and 7c
973 (Lower Sorling Valley) from Bentley et al (2007). The west coastline includes a
974 number of lateral moraines of the formerly more expansive Nordenskjöld Glacier
975 which may be related to the prominent inner basin moraine in the fjord. These
976 onshore lateral moraines are not dated but the inner basin moraine in the fjord can be

977 correlated based on geomorphological evidence to the inner basin moraine at the
978 entrance to Moraine Fjord, 2 km to the west (see Fig. 4). A cosmogenic isotope date
979 for this feature (GRE5, Bentley et al. 2007) had an unacceptably large error of 12900
980 ± 7800 yr BP so does not provide a reliable age constraint for these moraines. The
981 moraine from which sample GRE5 was collected has also been correlated on
982 geomorphological grounds with the Husvik medial moraine which had a weighted
983 mean cosmogenic isotope age of 12200 ± 1500 yr BP.

984

985 Appendix Figure A2. Multibeam swath bathymetry of Cumberland Bay West, South
986 Georgia combined with Figures 8a (Mercer Bay, Harpon Bay and Sphagnum Valley);
987 8b (Carlita Bay); 8c (Enten Bay); and the lower part of Figure 10b from Bentley et al
988 (2007). Although a shallow inner basin is not present on this image it is possible that
989 it may occur just south of Carlita Bay where Fig. 8b of Bentley et al. (2007)
990 documents a series of moraines and lake shorelines associated with an advance of the
991 Neumayer Glacier. These are undated.

992

993 Appendix Figure A3. Multibeam swath bathymetry of Stromness (upper image) and
994 Husvik (lower image) Harbours combined with Figure 18 of Bentley et al (2007)
995 which shows an overview of the geomorphology of Husvik Harbour, its major
996 moraine locations and interpreted ice marginal positions (I-III) that document
997 significant still stands during overall recession from the centre of the fjord. Combined,
998 these figures show the relationship between the onshore and offshore glacial
999 geomorphology including features from which age constraints from cosmogenic
1000 isotope exposure age dating and the onset of lake sedimentation are available.
1001 Radiocarbon ages from Block Lake and a soil profile south of Limit III are reported as

1002 the mean of the two-sigma range, calibrated using Calib 14C program v7.0 and the
1003 SHcal13 calibration curve. The terrestrial moraines in the inner basin of Husvik
1004 Harbour are interpreted as marking the oldest mapped ice advance on South Georgia
1005 based on a cosmogenic ^{10}Be exposure ages of between 14.2 and 10.6 ka BP, mean
1006 12.2 ± 1.5 ka BP, from the Husvik medial moraine (Bentley et al., 2007, 'category a'
1007 moraine). These 'category a' moraines have been correlated on geomorphological
1008 grounds with the oldest terrestrial moraine ridges in Antarctic Bay, Possession Bay
1009 and Moraine Fjord (Zenker Ridge) to the west of Cumberland Bay East (Appendix
1010 Figs. A4, A5, and A1, respectively).

1011

1012 Appendix Figure A4. Multibeam swath bathymetry of Antarctic Bay combined with
1013 Figure 14 of Bentley et al (2007) which is a geomorphological map of the west shore
1014 of Antarctic Bay. The oldest of the terrestrial moraines is a 'category a' moraines
1015 correlated on geomorphological grounds with the oldest terrestrial moraine ridges in
1016 Husvik Harbour Possession Bay and Moraine Fjord (Zenker Ridge) to the west of
1017 Cumberland Bay East (Appendix Figs. A3, A5, and A1, respectively).

1018

1019 Appendix Figure A5. Multibeam swath bathymetry of Possession Bay combined with
1020 Figure 16a of Bentley et al (2007) which is a geomorphological map of the valley on
1021 the south east shore of Possession Bay. This shows the outermost of a series of latero-
1022 frontal terrestrial moraine loops deposited by mountain ice to the south coalescing
1023 with the outer laterofrontal moraines of the former fjord ice and a prominent inner
1024 basin moraine in the fjord. This is a 'category a' moraine correlated on
1025 geomorphological grounds with the oldest terrestrial moraine ridges in Husvik

- 1026 Harbour, Antarctic Bay and Moraine Fjord (Zenker Ridge) to the west of Cumberland
1027 Bay East (Appendix Figs. A3, A4, and A1, respectively).

Table 1

Submarine glacial landforms	Royal Bay	Cumberland Bay East	Cumberland Bay West	Husvik Bay	Stromness Bay	Antarctic Bay	Possession Bay	King Haakon Bay	Drygalski Fjord	Age constraints based on terrestrial evidence
Inner basin	1	1	?	1	1	1	1	1	1	≤14.2 – 10.6 ka
Inner basin moraine	1	1	?	1	1	1	1	1	1	>14.2–10.6 ka >18.6 ka / LGM
Deep basin	1	1	1	1	1	1	1	1	1	<MIS 6
Deep basin moraine	?	1	?	1	1	0	1	?	1†	Earlier glaciation (MIS 6?)
Deep basin Truncated moraines/pro montories	4	3-4	2-4	1*	1	2	0	0	?	>MIS6
Cross shelf trough	1	1	1	0	0	1	1	1	1	>>MIS6

Table 1

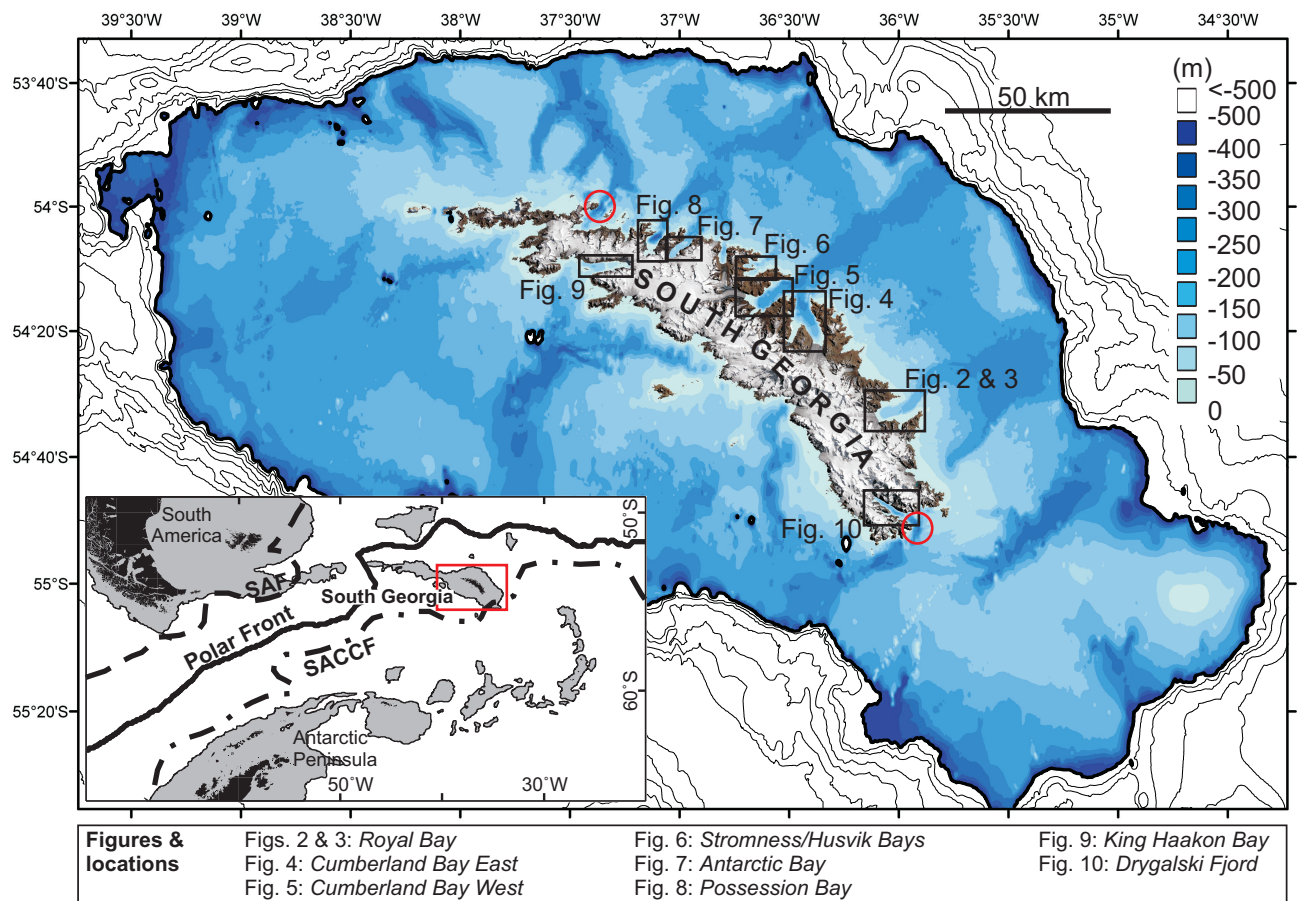


Figure 1, Hodgson et al.

*Figure 1B

[Click here to download high resolution image](#)



*Figure 2

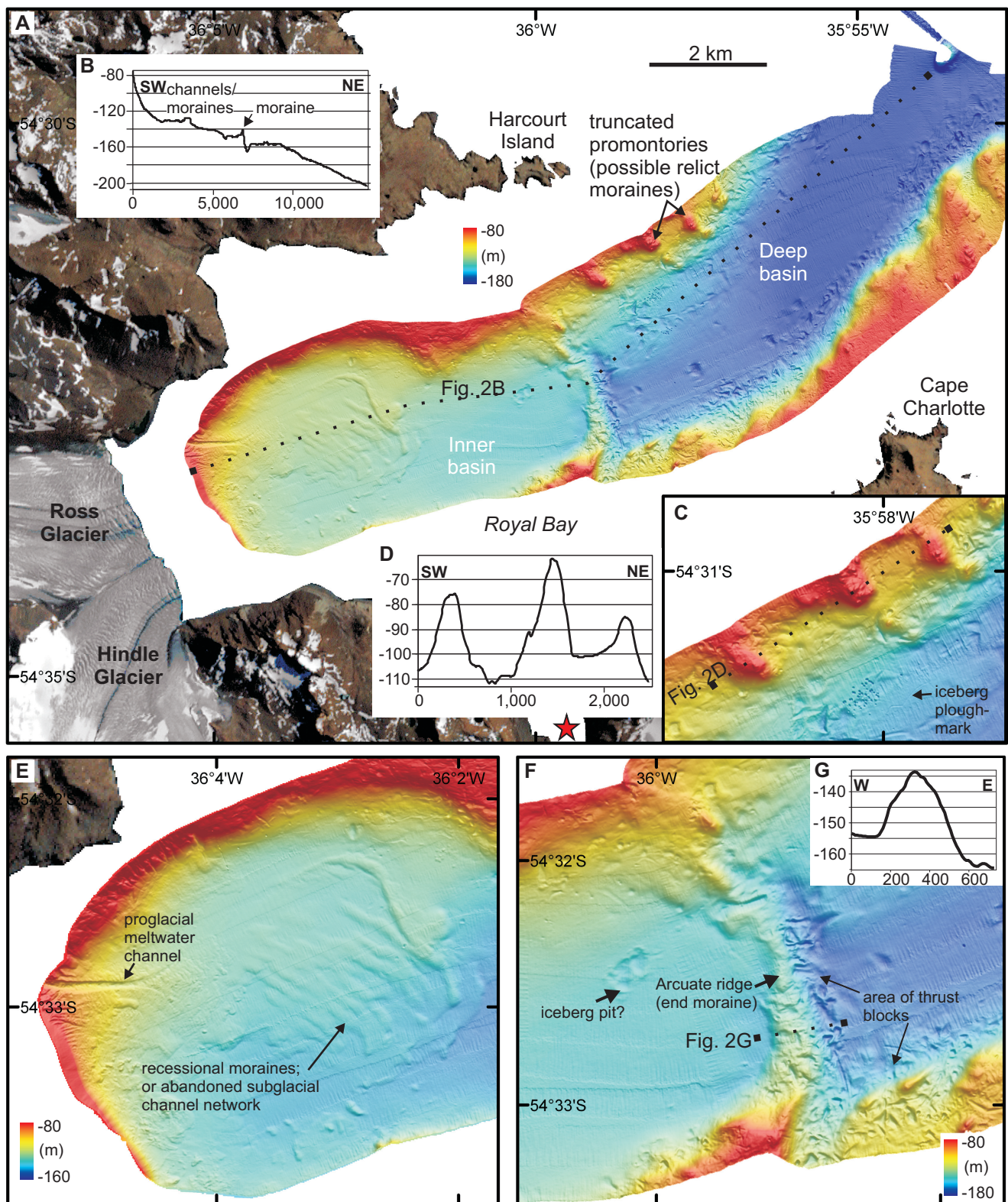


Figure 2. Hodgson et al.

***Figure 3**

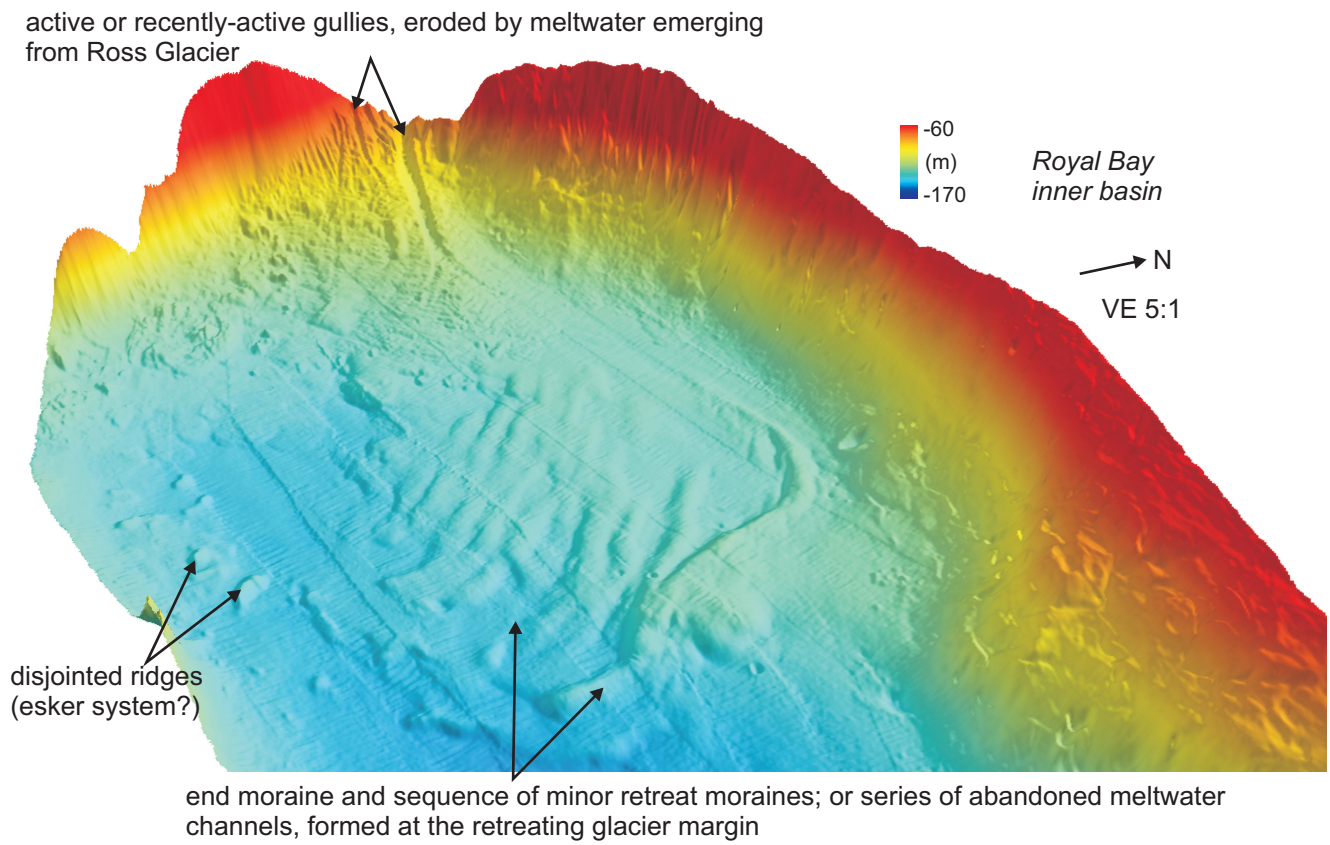


Figure 3. Hodgson et al.

*Figure 4

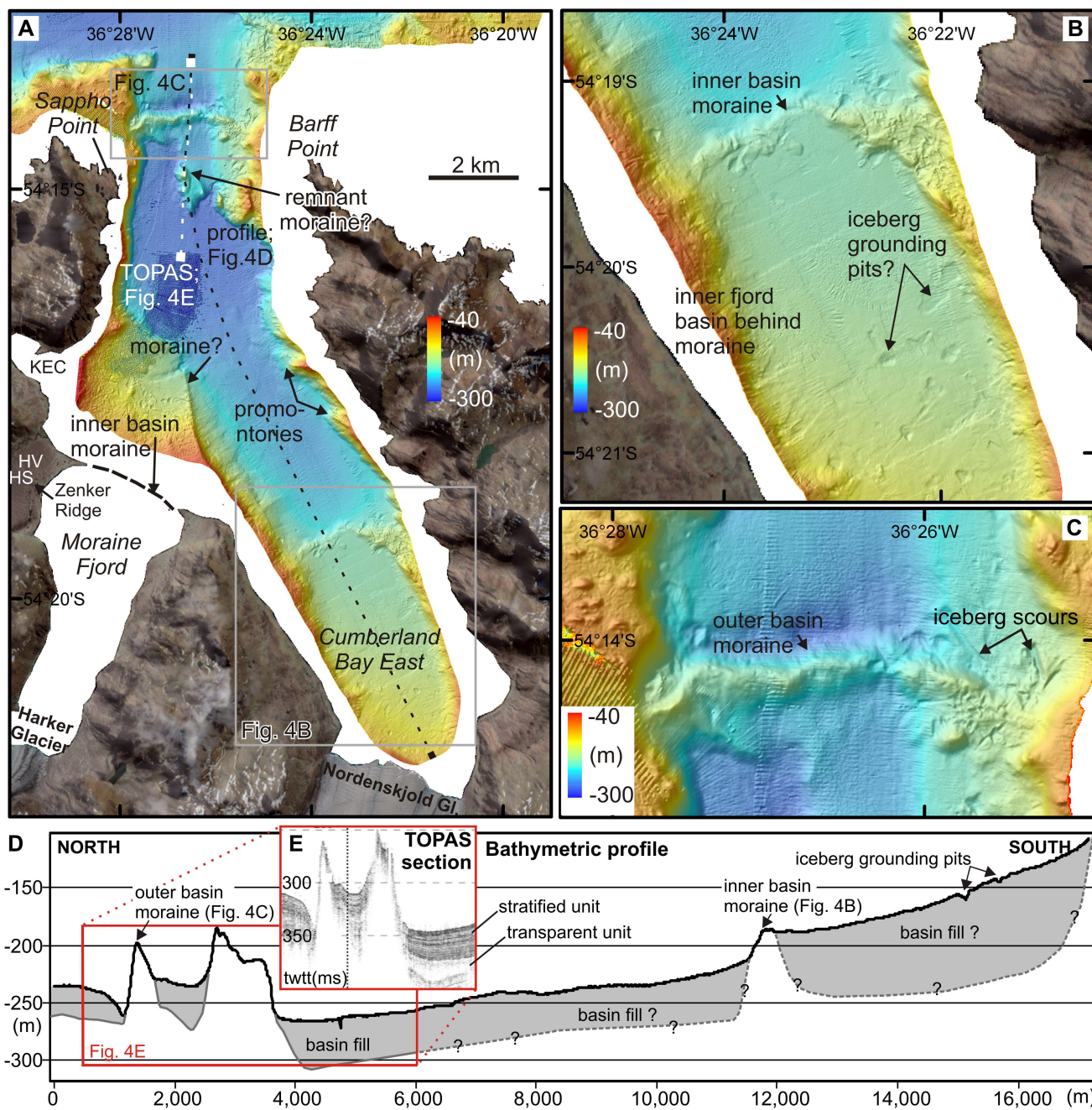


Figure 4, Hodgson et al.

*Figure 5

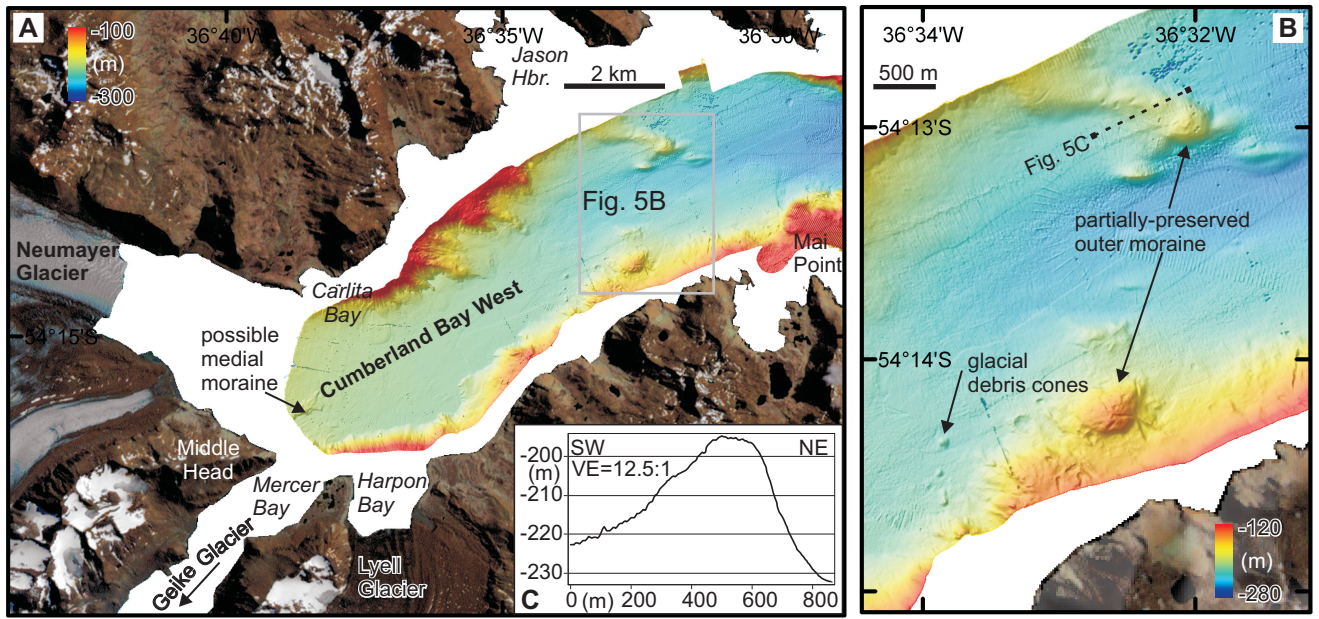


Figure 5, Hodgson et al.

*Figure 6A

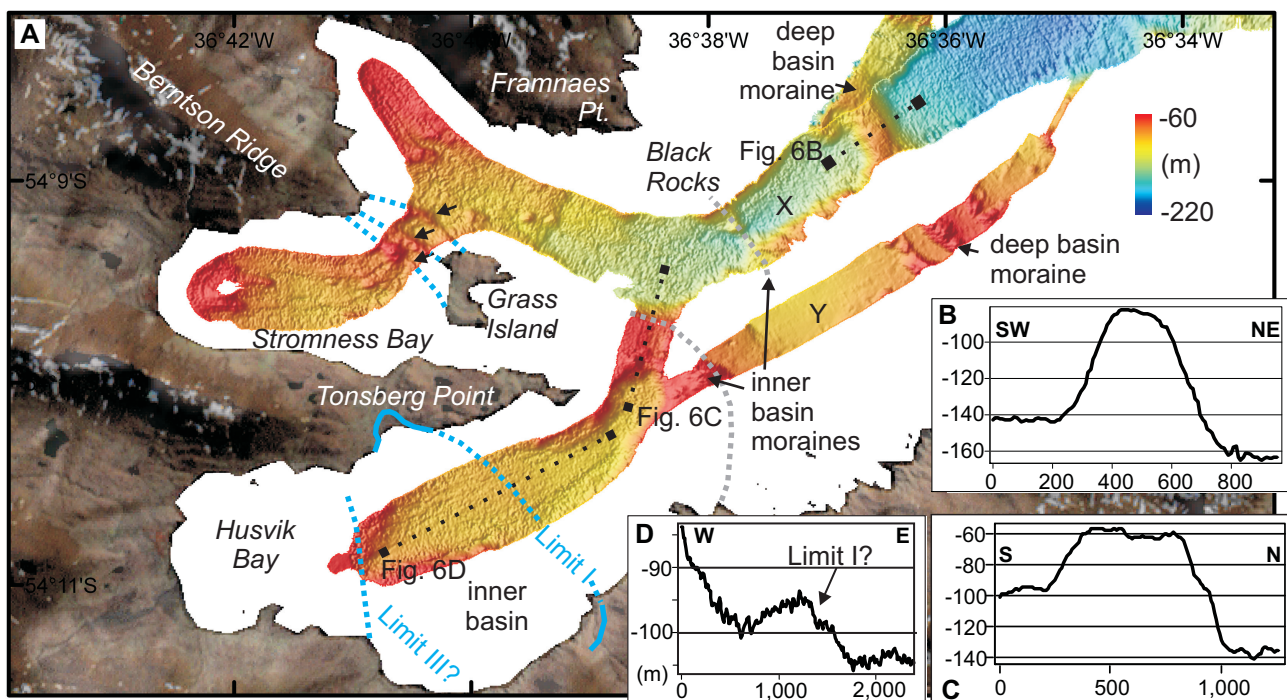


Figure 6, Hodgson et al.

*Figure 6B
[Click here to download high resolution image](#)



*Figure 7

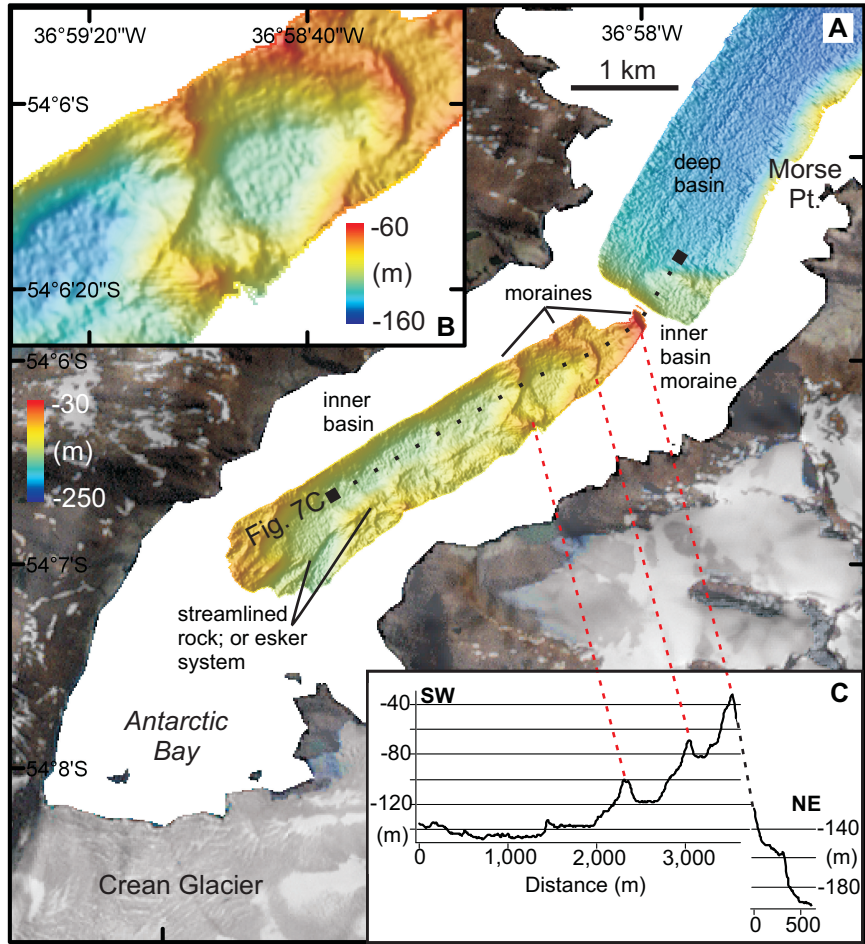


Figure 7, Hodgson et al.

*Figure 8

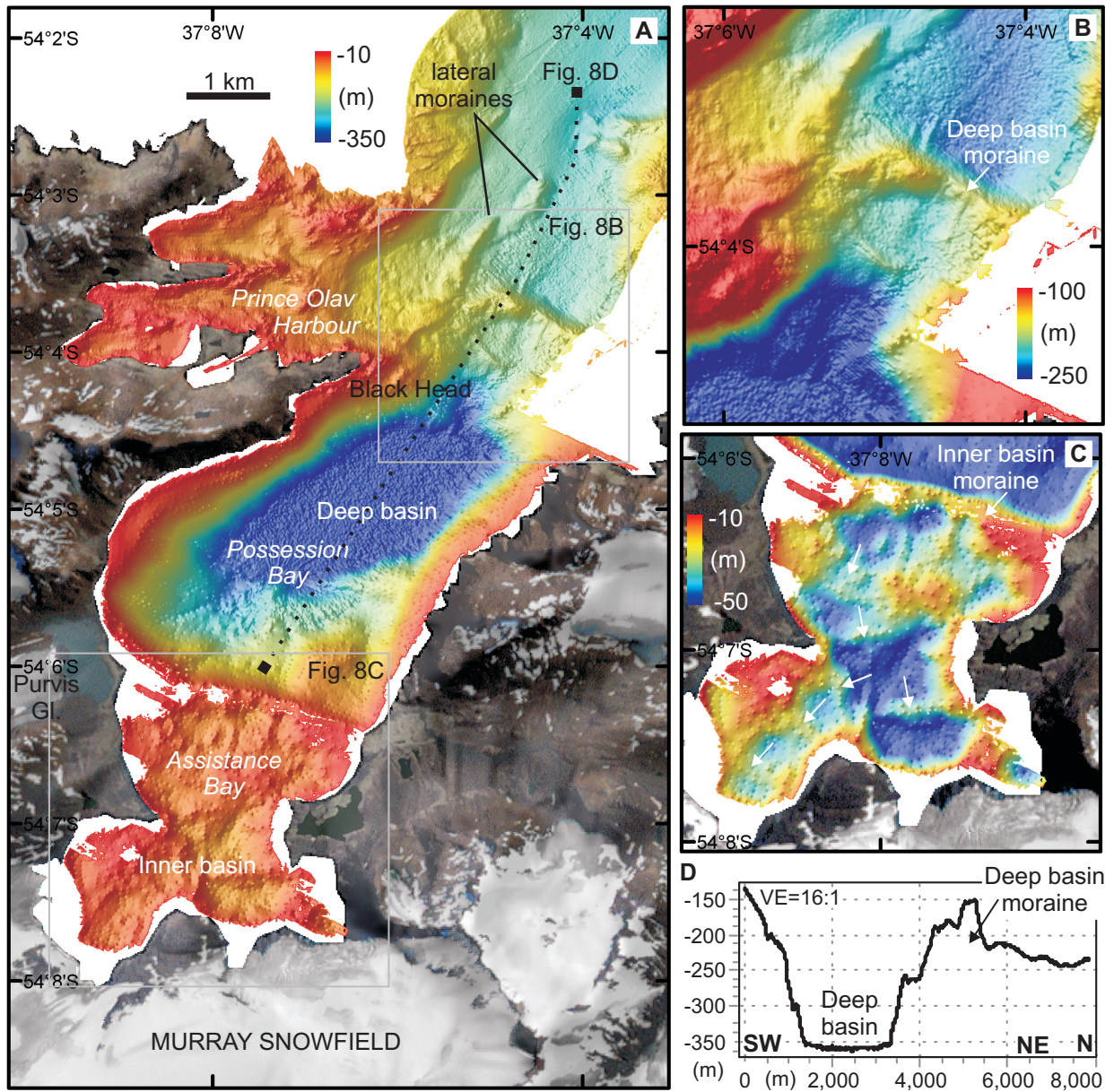


Figure 8, Hodgson et al.

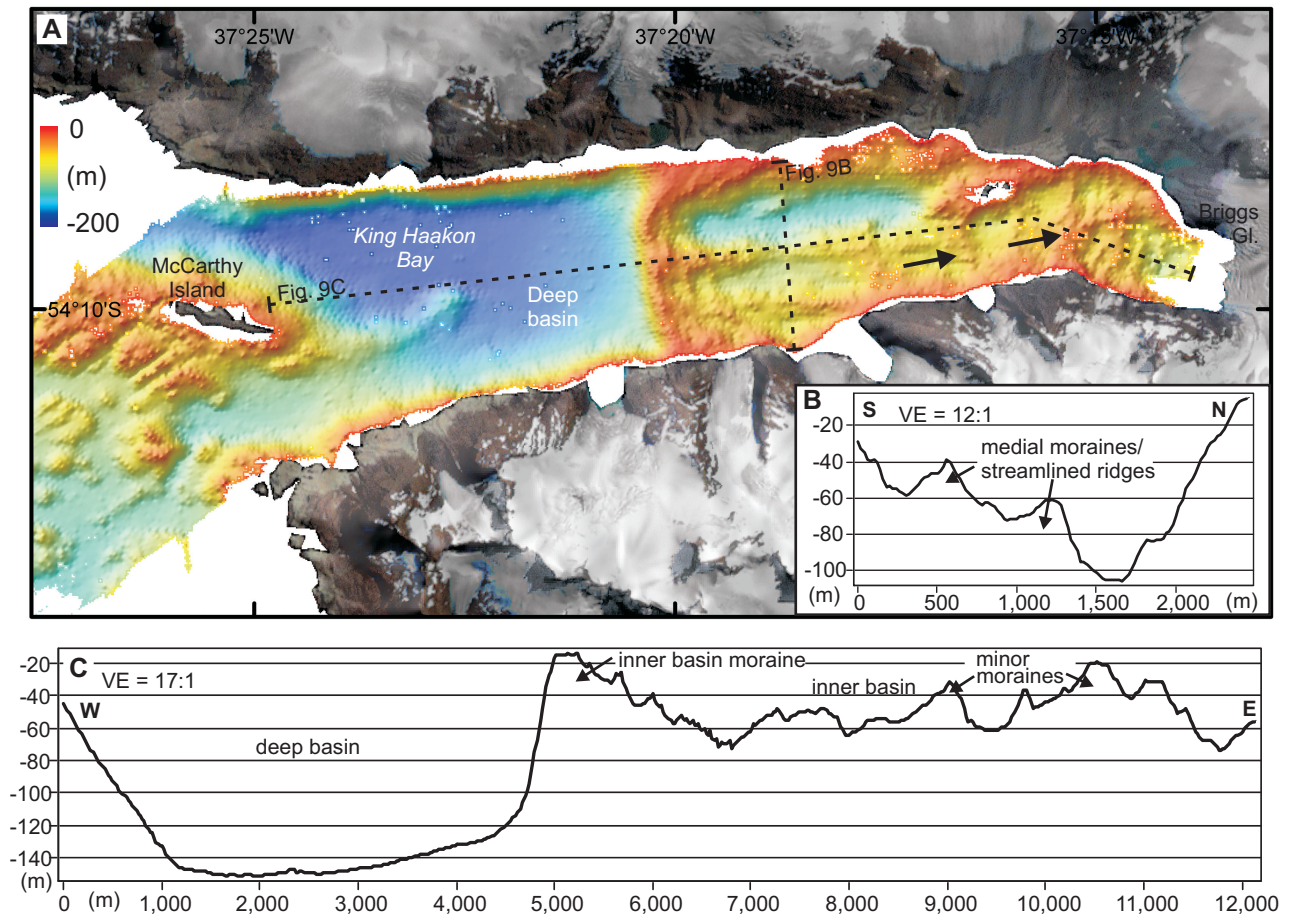


Figure 9, Hodgson et al.

*Figure 10

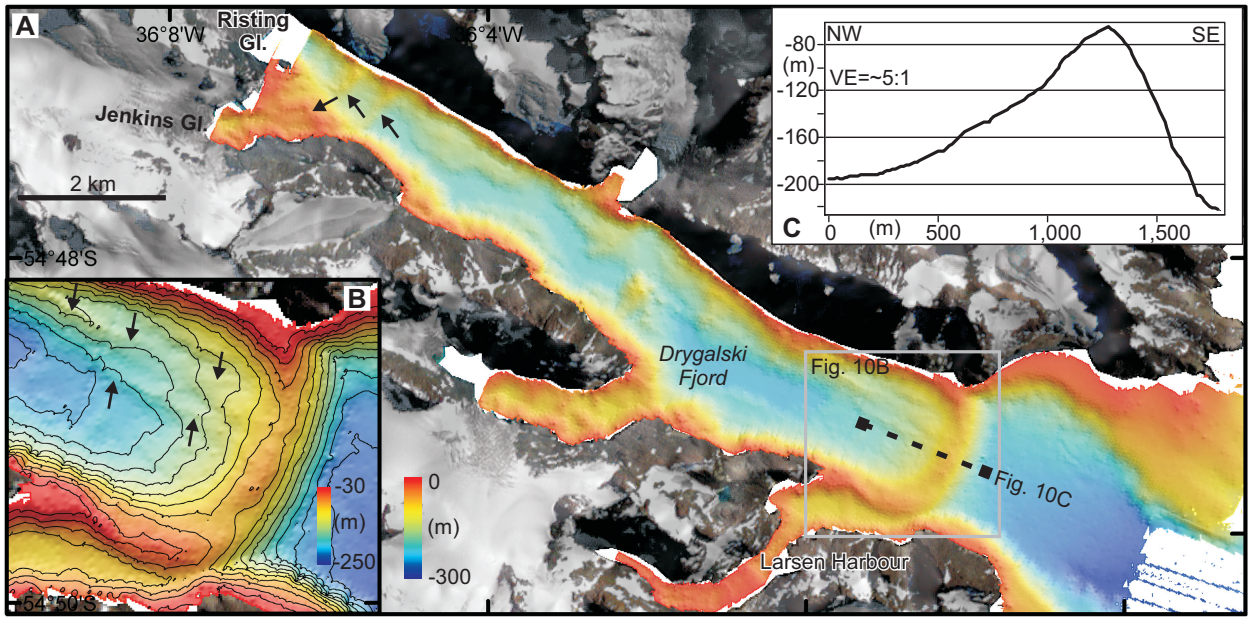


Figure 10. Hodgson et al.

*Figure 11

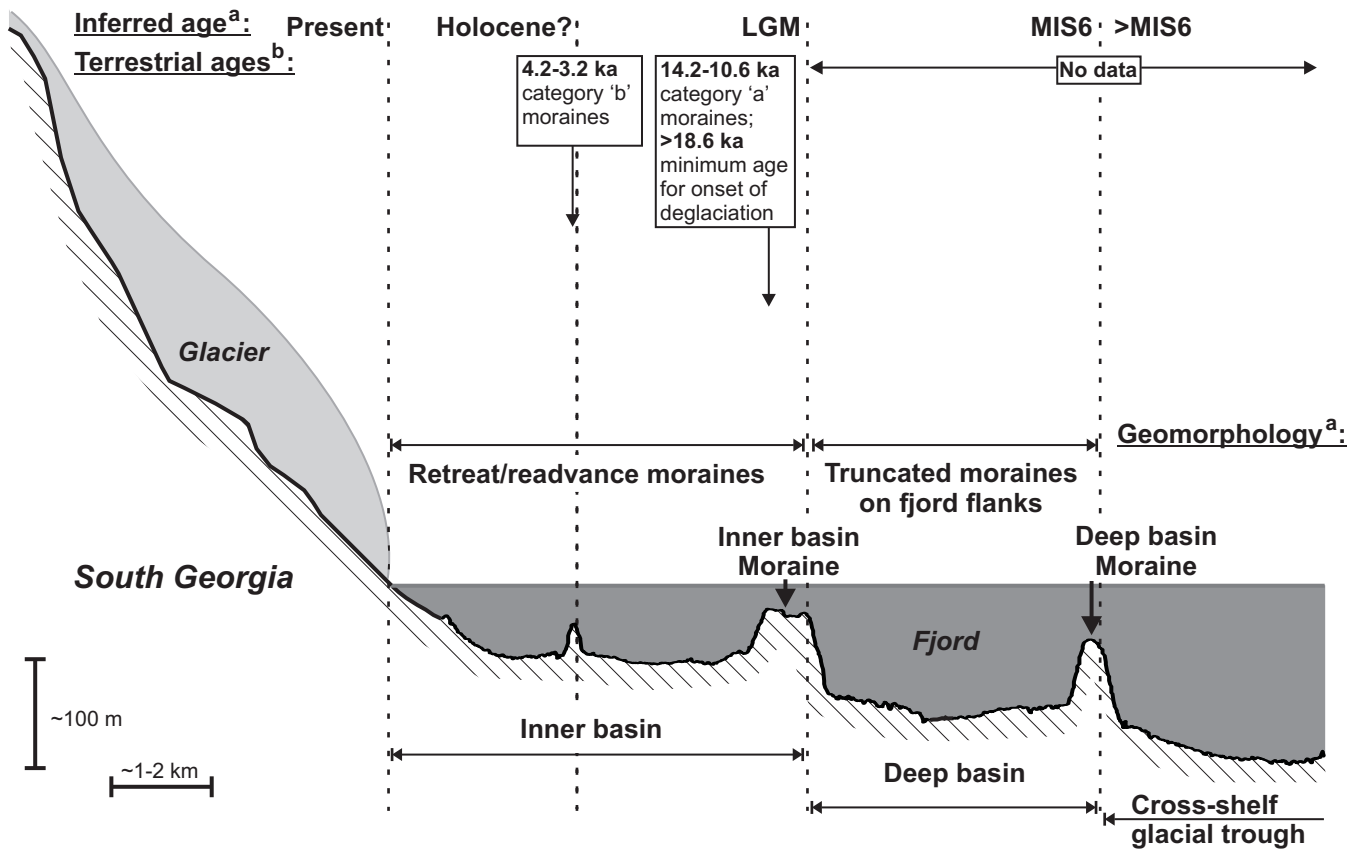
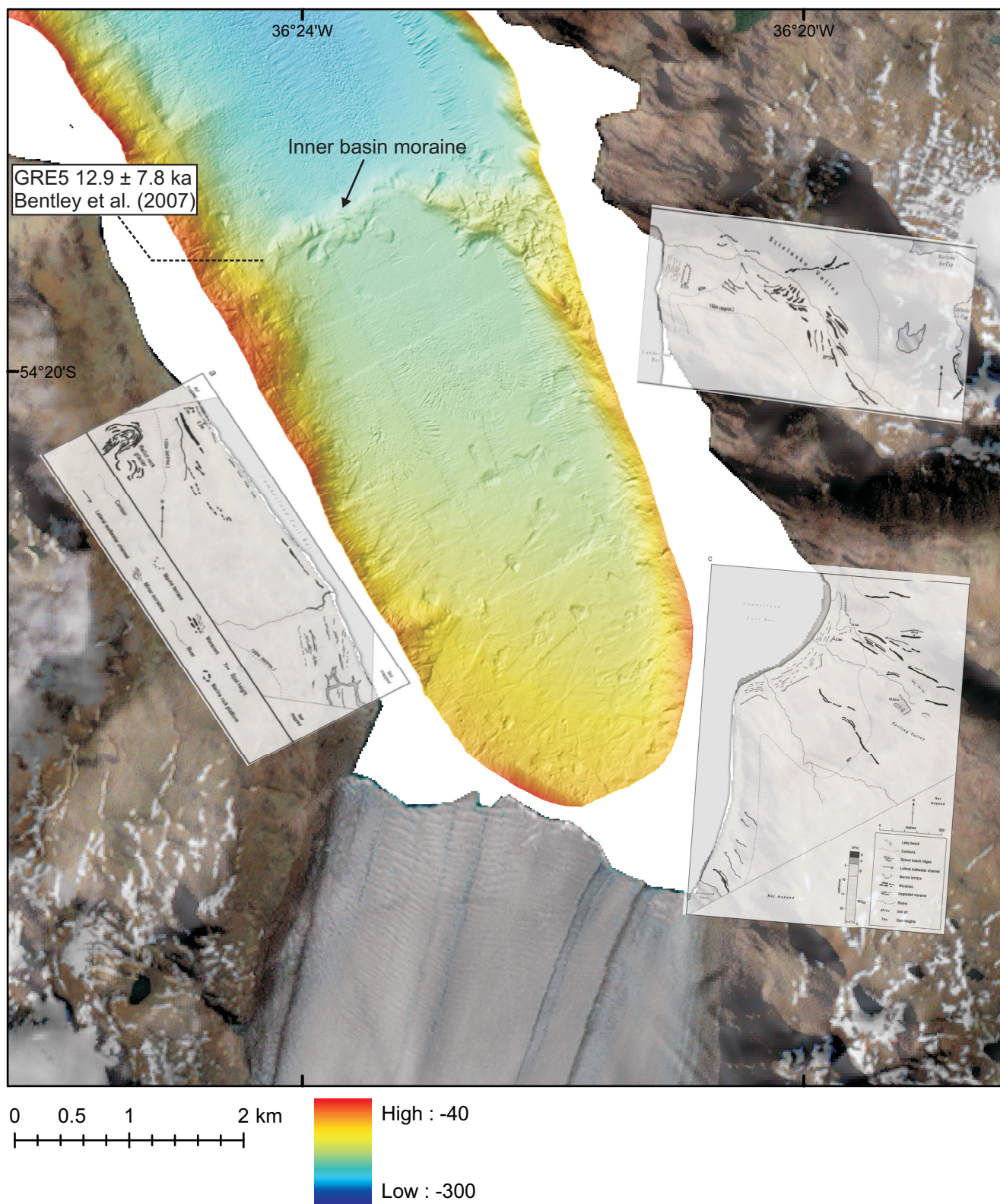


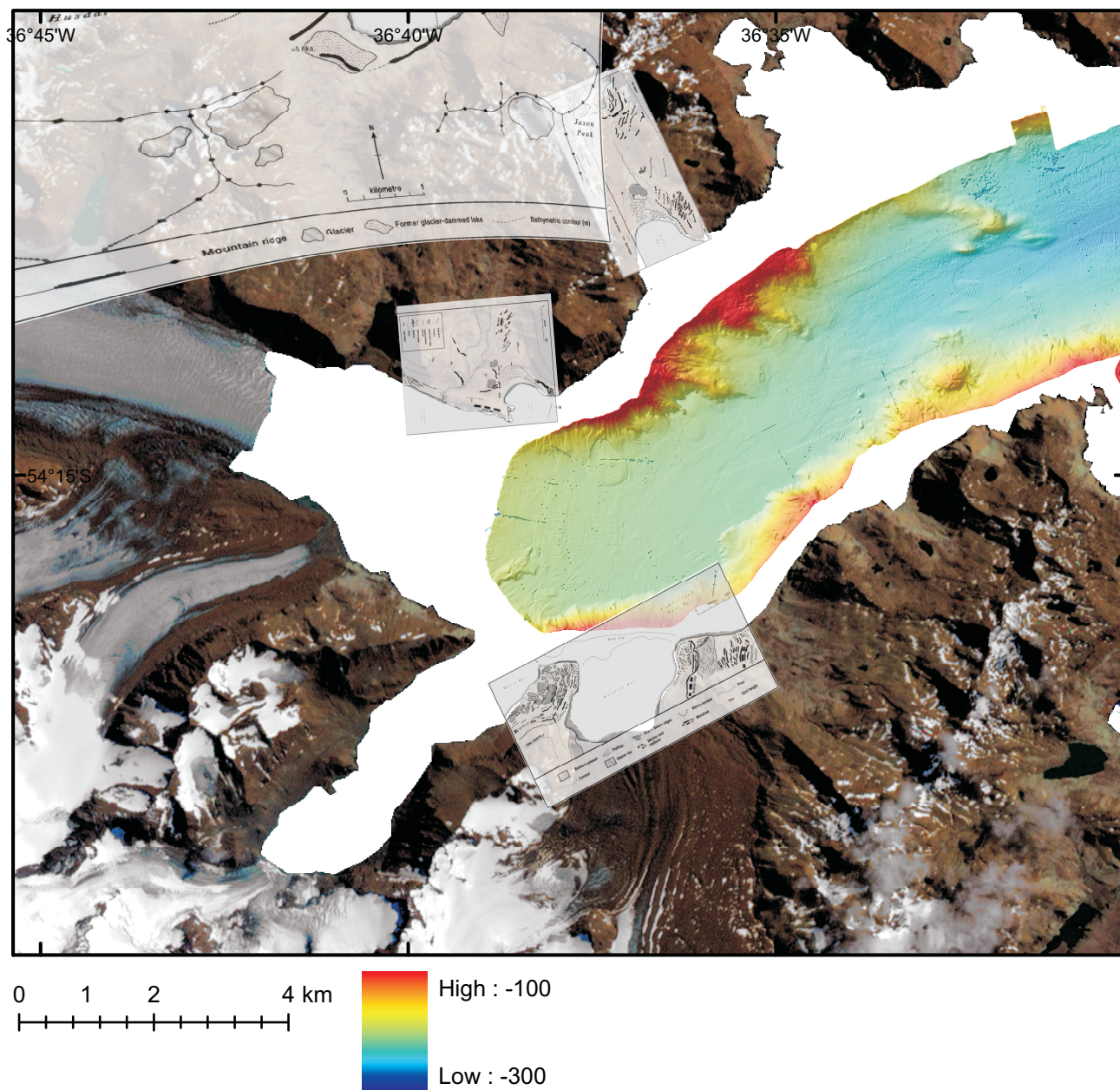
Figure 11, Hodgson et al.

*Figure Appendix A1



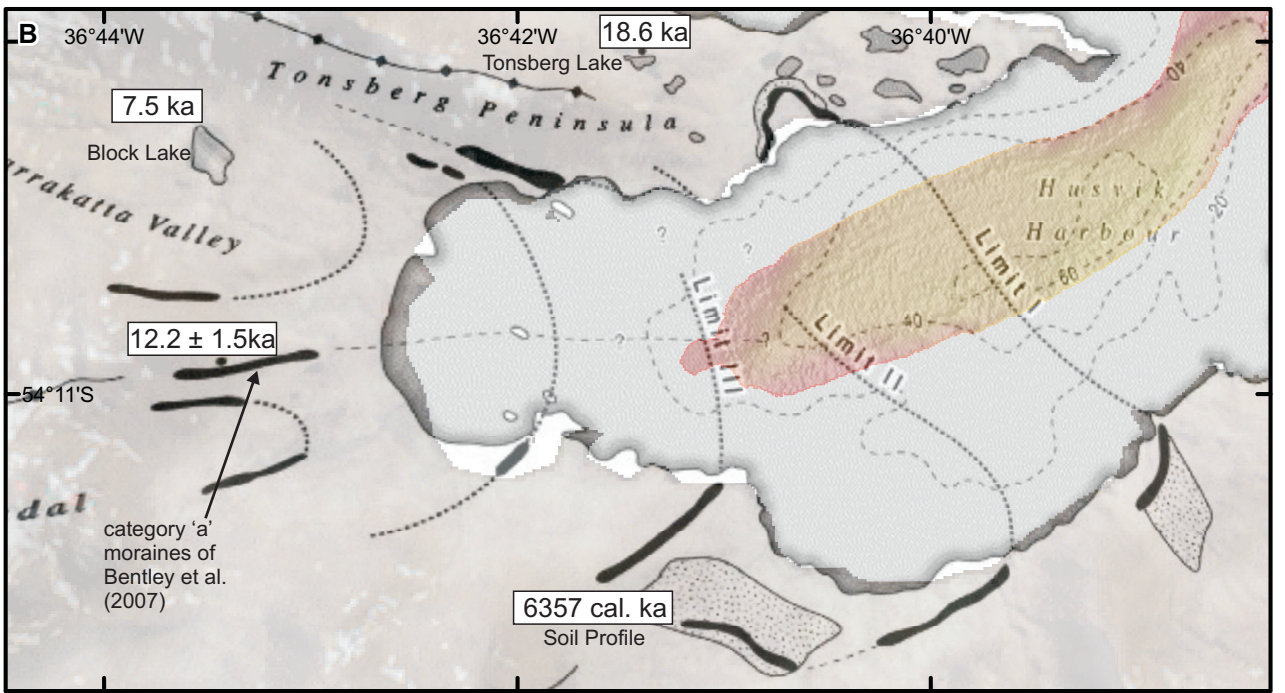
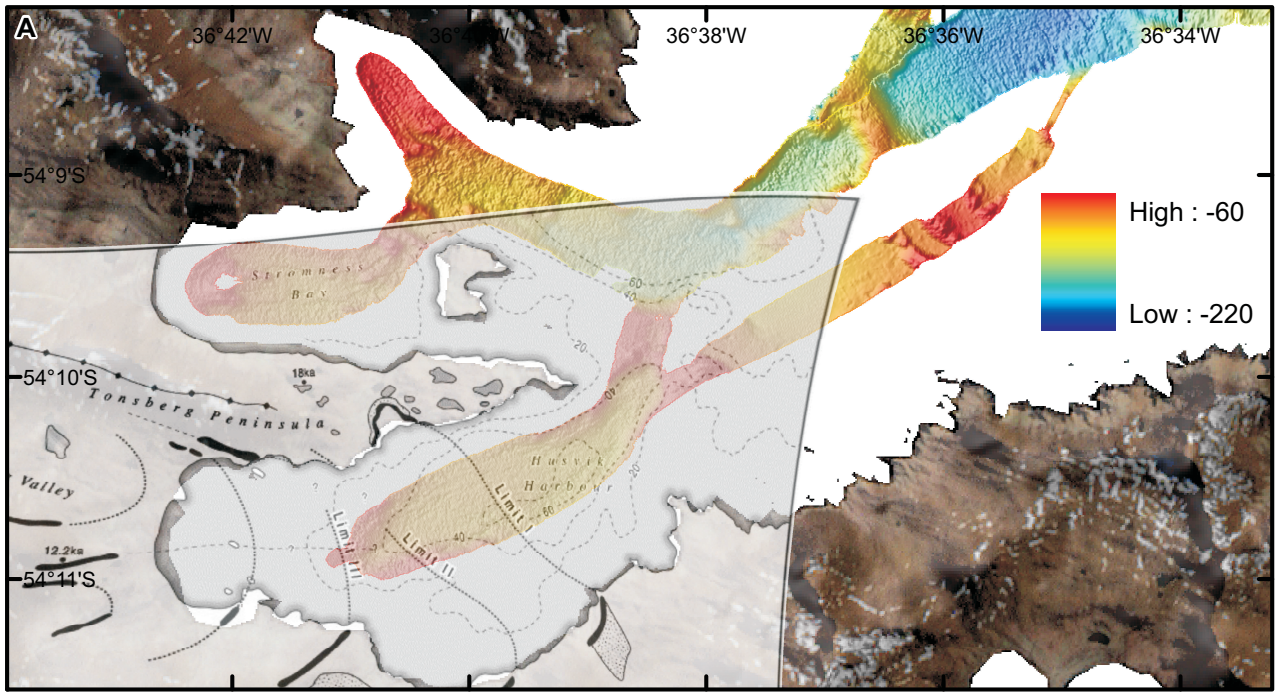
Appendix Figure A1

*Figure Appendix A2

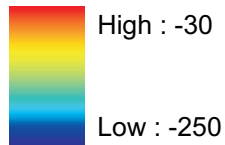
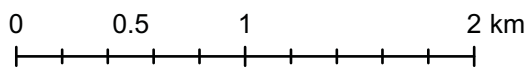
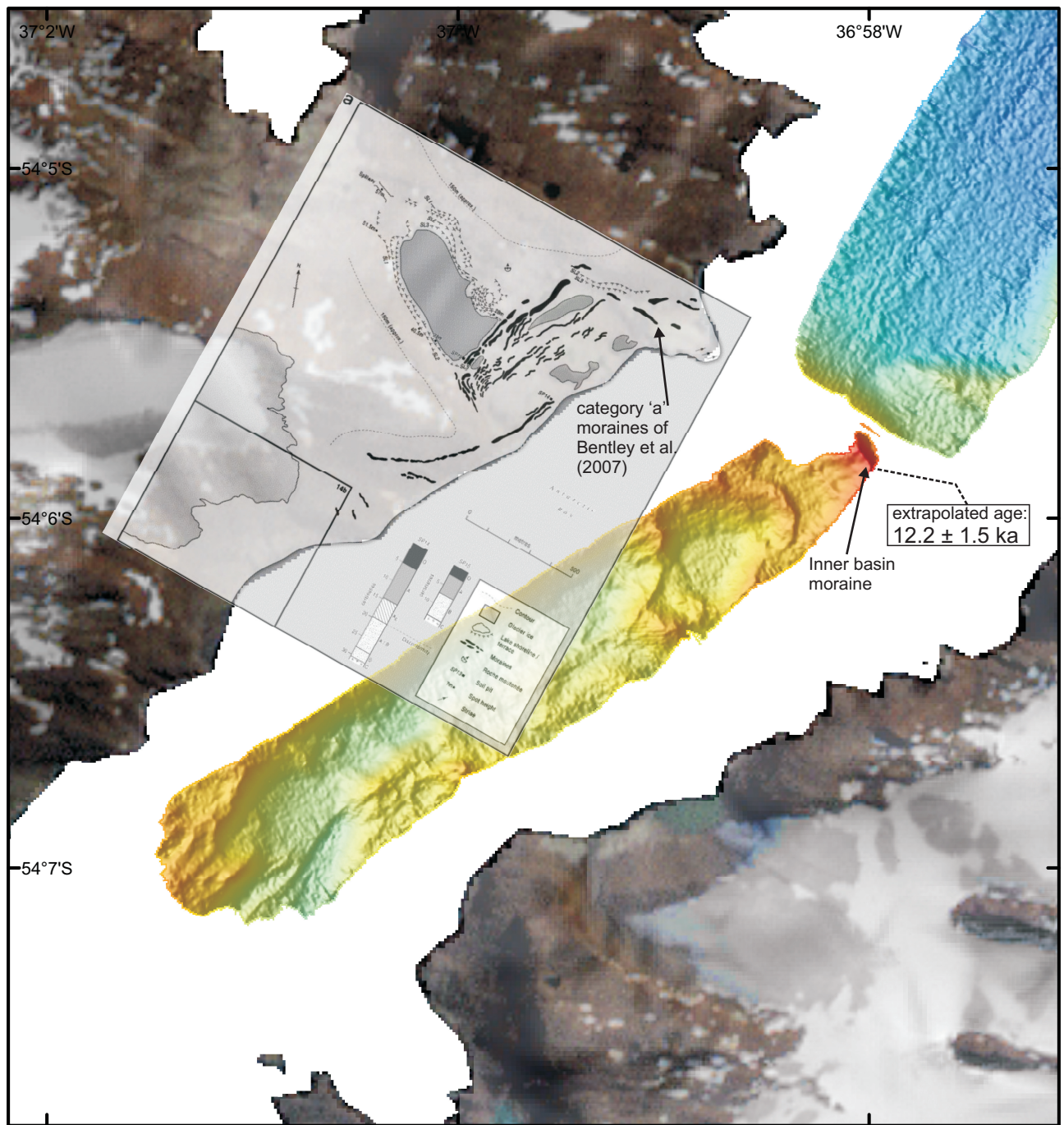


Appendix Figure A2

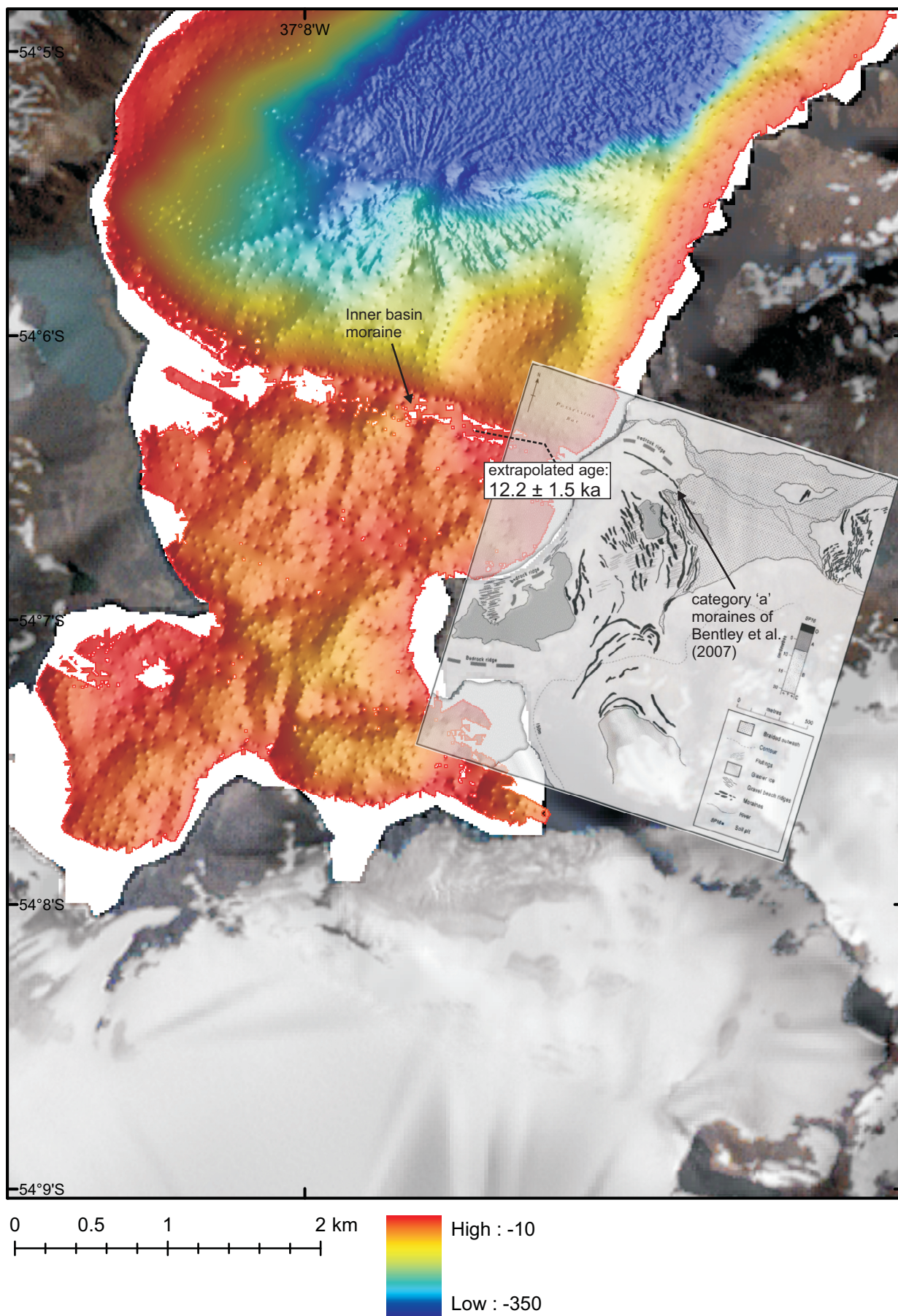
*Figure Appendix A3



Appendix Figure A3



Appendix Figure A4



Appendix Figure A5.